Bedford, Massachusetts

National Aeronautics and Space Administration
Headquarters
Washington, D. C. 20546

GCA CORPORATION
GCA Technology Division
Bedford, Massachusetts

Prepared by

Dr. F. F. Marmo, Project Director and
Principal Investigator

January 1965

EXPERIMENTAL AND THEORETICAL STUDIES IN PLANETARY AERONOMY

Quarterly Progress Report

Covering the Period 15 October 1964 thru
15 January 1965

Prepared under Contract No. NASw-840

TABLE OF CONTENTS

I. INTRODUCTION

This is the fifth in a series of reports which describes the technical progress under NASA Contract No. NASw-840 from 15 October 1964 through 15 January 1965.

For convenience and ease of reference, this report is divided into three sections. Section I summarizes the publications submitted or accepted for publication in accredited scientific journals as well as GCA Technical Reports generated and published during this reporting period. In Section II, the description of the technical progress follows the same order as outlined in the Statement of Work and each category is referenced respectively. Section III describes any additional work that was completed during the Quarter, but not necessarily required under the Statement of Work.

Scientific investigations accomplished during the current reporting period resulted in the generation of the following papers submitted and/or accepted for publication or presented at scientific meetings.

1. Technical Papers submitted and/or accepted for publication in accredited scientific journals for the period 15 October 1964 to 15 January 1965

	Journal
a. Submitted for publication	
On the Ozone Distribution in the Atmosphere of Mars (F. F. Marmo, ShardaNand and P. Warneck)	J. Geophys. Res.

	Journal
b. Accepted for Publication	
Ionospheric Electron Temperatures Near Dawn (A. Dalgarno and M. B. McElroy)	Planetary & Space Sciences
Absorption and Photoionization Cross Sections of CO_2, CO, A and He at Intense Solar Emission Lines (R. B. Cairns and J. Samson)	J. Geophys. Res.

2. Technical Papers presented at scientific or professional meetings during this Quarter

The Scattering of Lyman-Alpha Radiation (1215.6Å) by He, Ne, A, H_2 and N_2 (F. F. Marmo and Y. Mikawa) — Presented by Y. Mikawa at the American Physical Society Meeting, Chicago, Illinois, October 23-24, 1964.

3. Published GCA Technical Reports during this Quarter

	GCA TR No.
PLANETARY PHYSICS IX: A Congeries of Absorption Cross Sections for Wavelengths Less Than 3000Å. II (J. O. Sullivan and A. C. Holland [December 1964]	64-20-N

II. TECHNICAL PROGRESS ON ITEMS APPEARING IN THE STATEMENT OF WORK

In this section, we report only those items that are listed in the Statement of Work. For convenience and ease of reference, each topic is discussed in the order in which it appears in the Work Statement.

A. SOLAR PHOTOLYSIS OF PLANETARY GASES

There are four tasks listed in the Work Statement under solar photolysis of planetary gases which are designated as Items A-1, A-2, A-3 and A-4. These will be discussed in the order in which they appear in the Statement of Work.

CO_2 Photolyses at 1470Å, 1236Å, 1066Å and 1600Å (Ref. Work Statement, Items A-1, A-2, A-3 and A-4, respectively)

Statement of Work Items A-1, A-2 and A-4 have been completed and have resulted in the following publications:

(a) "Reactions of ^1D Oxygen Atoms in the Photolysis of Carbon Dioxide. I" [P. Warneck, GCA TR No. 64-7-N and Discussions of Faraday Society, No. 37, 57-65, 1964].

(b) "Reactions of ^1D Oxygen Atoms in the Photolysis of Carbon Dioxide. II" [P. Warneck, GCA TR No. 64-15-N and J. Chem. Phys. 41, No. 11, 3435-3439, 1 Dec 1964].

The work accomplished is described in complete detail in the above publications so that no further description is necessary to include in the

present write-up. In any case, it appears that since the CO_2 photolyses for the spectral regions 1470Å, 1236Å and 1600Å have been completed, the remaining task is to study the photochemical behavior of CO_2 subjected to radiation in the 1066Å region (Reference Work Statement, Item A-3).

Under the present study, this is to be accomplished by employing a novel argon resonance light source with emission lines at 1048Å and 1066Å. This light source has been designed, constructed and tested during this Quarter. Although spectral purity was achieved, some difficulty was encountered in employing this light source with a LiF window. For example, since the argon resonance lines at 1048 and 1066Å lie very close to the transmission cutoff for LiF, not only was a substantial portion of the resident radiation absorbed but in addition, the LiF transmissivity decreased sharply with time. As a consequence, this restricted the irradiation dosage; i.e., the total number of quanta.

Some effort was devoted toward determining the nature of this behavior. Surprisingly enough, it was found that these phenomena could be associated with the formation of color centers due to absorption by the LiF fundamental band. Unfortunately, this implied a more or less permanent damage to the window employed so that it was not possible to restore the LiF transmissivity by mere chemical cleansing. It was further determined that with the present setup, the irradiation dosage is limited to no more than 10^{17} quanta. Accordingly, appropriate modifications had to be devised in order to increase the sensitivity of the system so that reliable data could be obtained with this relatively small dose. It was decided to

design a small volume reactor and fit it with a LiF window in such a manner that the unit could simultaneously serve as the sampling cell. In this way, losses in transfer of the irradiated samples are avoided. Thus, it appears that even with the limited irradiation dosage of only 10^{17} quanta, the current modifications will allow evaluation of product concentrations by conventional mass spectrometric techniques so that reliable results should be forthcoming within the next Quarter although this is not as yet a certainty.

B. THEORETICAL STUDIES

There are four tasks listed in the Work Statement under theoretical studies which are designated as Items B-1, B-2, B-3 and B-4. These will be discussed in the order in which they appear in the Statement of Work.

Quantum Calculations of the Photoionization Cross Sections of Atomic Oxygen Taking Account of the Individual Transitions (Ref. Work Statement, Item B-1)

This phase of the work has been completed and is described in detail in the following publications:

(a) "The Photoionization of Atomic Oxygen" [A. Dalgarno, R. Henry and A. Stewart, GCA TR No. 64-1-N and Planetary & Space Sciences 12, 235, 1964].

The Determination of Electron Temperatures in the Upper Atmosphere With Special Emphasis on the Near Sunrise Period (Ref. Work Statement, Item B-2)

This phase of the work has been completed and is described in detail in the following publication:

(a) "Ionospheric Electron Temperatures Near Dawn" [A. Dalgarno and M. B. McElroy, Planetary & Space Sciences, to be published].

Determination of the Cooling of Electrons by Rotational Excitation of Molecular Nitrogen in the D Region (Ref. Work Statement, Item B-3)

This is the only remaining theoretical task to be performed under the work statement requirement. Accordingly, considerable progress has been

achieved during the past Quarter toward completing this phase of the work. Since no definite and final results are yet available, no description of the work accomplished to date is given here; however, it is felt that this will be completed under the present contract.

The Improved Calculations of the Ambi-Polar Diffusion Coefficient Appropriate to the F-Region (Ref. Work Statement, Item B-4)

This phase of the work has been completed and is described in detail in the following publication:

(a) "Ambipolar Diffusion in the F-region" [A. Dalgarno, J. Atmos. Terrest. Phys., to be published].

C. EXPERIMENTAL INVESTIGATIONS IN THE VUV (1000-2000Å) AND EUV (BELOW 1000Å)

There are four tasks listed in the Work Statement under experimental investigations of the EUV and VUV which are designated as Items C-1, C-2, C-3 and C-4. Each task is discussed in the order in which it appears in the Statement of Work.

Measurement of Absorption and Photoionization Cross Sections in the VUV and EUV Regions for O_2, N_2 and A (Ref. Work Statement, Item C-1)

This phase of the work has been completed and is described in detail in the following publications:

(a) "Absorption and Photoionization Cross Sections of O_2 and N_2 at Intense Solar Emission Lines" [J. Samson and R. B. Cairns, J. Geophys. Res., 1 Nov 1964].

(b) "Absorption and Photoionization Cross Sections of CO_2, CO, A and He at Intense Solar Emission Lines" [R. B. Cairns and J. Samson, J. Geophys. Res., 1 Jan 1965].

(c) "Experimental Photoionization Cross Sections in Argon from Threshold to 280Å" [J. Samson, GCA TR No. 64-3-N and J. Opt. Soc. Amer., 54, 420, 1964].

(d) "Photoionization of the Rare Gases" [J. Samson, GCA TR No. 64-3-N].

(e) "Absorption and Photoionization Cross Sections of Atmospheric Gases at Intense Solar Emission Lines: N_2, O_2, CO_2, CO, A and He" [J. Samson, R. B. Cairns and F. L. Kelley, GCA TR No. 64-13-N, Sept 1964].

Laboratory Measurements of Absorption and Photoionization Cross Sections of Atomic Oxygen, Atomic Nitrogen and Atomic Hydrogen (Ref. Work Statement, Item C-2)

In the last report, the technique to be used in this experiment was briefly described and the methods of producing atomic oxygen and measuring its quantity were given.

At that time it was thought that only ground-state oxygen atoms and molecules were present in appreciable quantities in the gas flowing out from the discharge region. This supposition was based on a paper by Linnett and Marsden (Proc. Roy. Soc. A234, 489, 1956) who gave evidence discounting the presence of atomic and molecular ions, ozone, electronically-excited oxygen molecules or atoms, and vibrationally-excited molecules in the gas downstream from the r.f. discharge. This work was supported by Neynaber et al. (Phys. Rev. 123, 149, 1961) and Fite and Brackmann (Phys. Rev. 113, 815, 1959). However, a recent paper by Bader and Ogryzlo (Faraday Society Meeting, 1964) states that species present in electronically-discharged oxygen are $O_2(^3\Sigma_g^-)$; O; $O_2(^1\Delta_g)$; $O_2(^1\Sigma_g^+)$ in approximate ratios 1 : 0.1 : 0.05 : 0.0015. The evidence for the existence of $O_2(^1\Delta_g)$ is indirect. However, if present, its concentration remains high downstream from the discharge.

In our experiments it was necessary (a) to determine whether excited molecular states were present and (b) if present, to make allowance for the contribution of these species to the total light absorbed.

(a) Excited molecular states were present. They were detected in the following manner. Radiation in the wavelength region 1250 to 950Å was partially absorbed by ground state O_2. The O_2 was then discharged upstream from the absorption cell. If ground state O_2 and O were the only species formed, the light should be less absorbed since O does not absorb continuously at wavelengths longer than 910Å. However, at certain wavelengths there was increased absorption which indicated the presence of other species with absorption cross sections greater than ground state O_2. Neither the nature of these species nor their concentrations were determined although the major one was probably $O_2(^1\Delta_g)$.

(b) To measure the absorption cross section of O in the presence of both $O_2(^3\Sigma_g^-)$ and $O_2(^1\Delta_g)$, it was necessary to remove, selectively, either the O atoms or the $O_2(^1\Delta_g)$. Several techniques for the removal of oxygen atoms have been employed. The method most successful for the removal of O while not deactivating $O_2(^1\Delta_g)$ is the presence of mercuric oxide in the flow tube. This was reported by Bader and Ogryzlo (Faraday Society Meeting, 1964) who prepared the mercuric oxide by the distillation of mercury through a discharge in O_2.

The revised experimental technique, using mercuric oxide to remove only O, is described below with the appropriate equations.

If discharged oxygen containing

$O_2(^3\Sigma_g^-)$; number density $n'_{(O_2)}$; absorption cross section $\sigma_{(O_2)}$;

$O_2(^1\Delta_g)$; " " $n_{(O_2^*)}$; " " " $\sigma_{(O_2^*)}$;

and O; number density $n'_{(O)}$; absorption cross section $\sigma_{(O)}$; transmits light of intensity I'; then,

$$I' = I_o \exp - [\sigma_{(O_2)}\, n'_{(O_2)}\, L + \sigma_{(O_2^*)}\, n_{(O_2^*)}\, L + \sigma_{(O)}\, n'_{(O)}\, L] \quad (1)$$

where I_o is the incident light intensity and L the length of the absorbing column.

If mercuric oxide now removes nearly all of the O leaving a concentration $n''_{(O)}$; and $n_{(O_2^*)}$ remains constant then,

$$I'' = I_o \exp - [\sigma_{(O_2)}\, n''_{(O_2)}\, L + \sigma_{(O_2^*)}\, n_{(O_2^*)}\, L + \sigma_{(O)}\, n''_{(O)}\, L]. \quad (2)$$

But if $N_{(O_2)}$ was the initial number of O_2 molecules per cc before the discharge was switched on,

$$N_{(O_2)} = n'_{(O_2)} + n_{(O_2^*)} + \tfrac{1}{2}\, n'_{(O)} \quad (3)$$

$$= n''_{(O_2)} + n_{(O_2^*)} + \tfrac{1}{2}\, n''_{(O)} \quad . \quad (4)$$

Using Equations (1), (2), (3) and (4)

$$\sigma_{(O)} = \tfrac{1}{2}\, \sigma_{(O_2)} - \frac{1}{L(n'_{(O)} - n''_{(O)})} \ell n \frac{I'}{I''} \quad . \quad (5)$$

In this expression $\sigma_{(O_2)}$, L, $n'_{(O)}$, $n''_{(O)}$, I' and I'' are measured quantities.

Atomic cross sections have been measured using Equation (5) and are plotted in Figure 1 together with the theoretical curve of Dalgarno et al. (GCA Technical Report No. 64-1-N, 1964). These data are preliminary. An

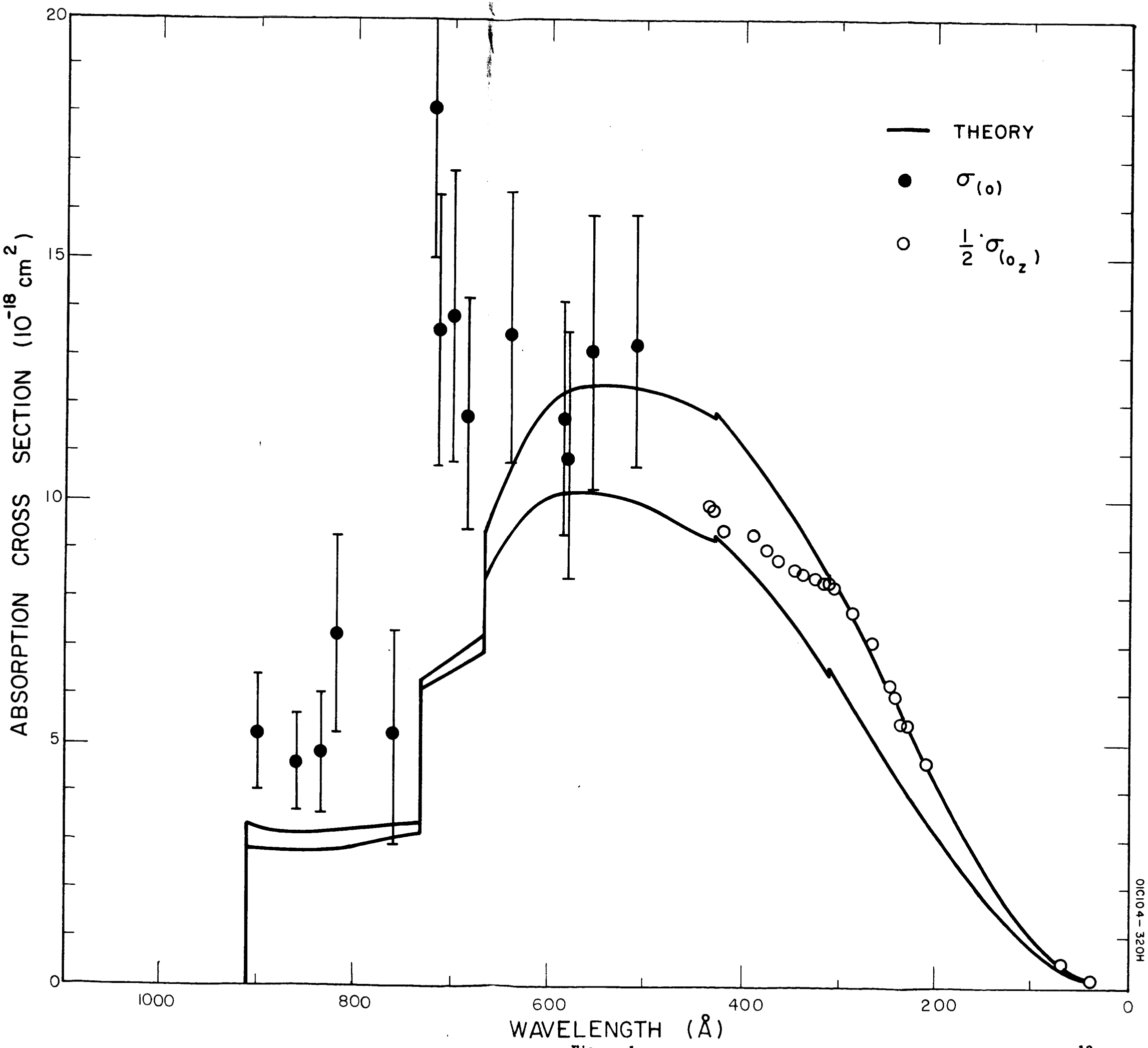
THEORY
$\sigma_{(o)}$
$\frac{1}{2}\cdot\sigma_{(o_z)}$
ABSORPTION CROSS SECTION (10^{-18} cm^2)
20
15
10
5
0
1000
800
600
400
200
0
WAVELENGTH (Å)
01C104-320H

Figure 1.

estimate of the probable errors requires more data which will become available within the next month. However, it appears that the experimental results will be in broad agreement with theory, being higher by less than 50 percent.

Extremely high cross sections are obtained at certain wavelengths, for example 725Å. There are two possible explanations:

(1) autoionization, and

(2) at this particular wavelength $\sigma_{(O_2^*)} \ll \sigma_{(O_2)}$.

This being so, any deactivation of $O_2(^1\Delta_g)$ by the mercuric oxide (for which account has not been taken) would increase the apparent value of $\sigma_{(O)}$. The most accurate values of $\sigma_{(O)}$ are obtained when $\sigma_{(O_2^*)} \cong \sigma_{(O_2)}$. This is probably so for $\lambda < 600$Å.

Summary:

(1) The presence of species other than ground state O_2 and O have necessitated revised techniques.

(2) Such techniques have been utilized and preliminary data obtained.

(3) The probable errors associated with the data have yet to be finally assessed but are of the order of ± 30%.

(4) To complete the investigations, the following experiments would be desirable:

   (a) To obtain the photographic absorption spectrum of oxygen atoms in order to search for the expected autoionization levels.

(b) To obtain direct evidence for the existence of $O_2(^1\Delta_g)$ by measuring the ionization onset of the discharged products. The relative absorption cross sections of $O_2(^1\Delta_g)$ can be calculated from the data already obtained if this is the only significant constituent in addition to $O_2(^3\Sigma_g^-)$ and O.

Laboratory Measurements of the Kinetic Energies of Photoelectrons From N_2 and O_2 (Ref. Work Statement, Item C-3)

Since the majority of photoelectrons are released at right angles to the photon beam, an elementary electron analyzer can be constructed using a parallel plate configuration. With the collector plate held at a negative potential, ions will always be collected as well as electrons with energies greater than the negative voltage applied to the collector. As this potential is increased, fewer electrons are collected and the total current increases to a maximum value. At this point the applied voltage is equal to the electron energy E (see Fig. 2). As the voltage is further increased and the electrons gain more energy, secondary ionization of the gas by the electrons is possible and the current again increases.

This technique has been used successfully with the rare gases and the plateau always starts at

$$E = h\nu - I.P.$$

The rise at higher voltages has been confirmed. However, using O_2, N_2 and CO_2, very little secondary ionization takes place indicating that

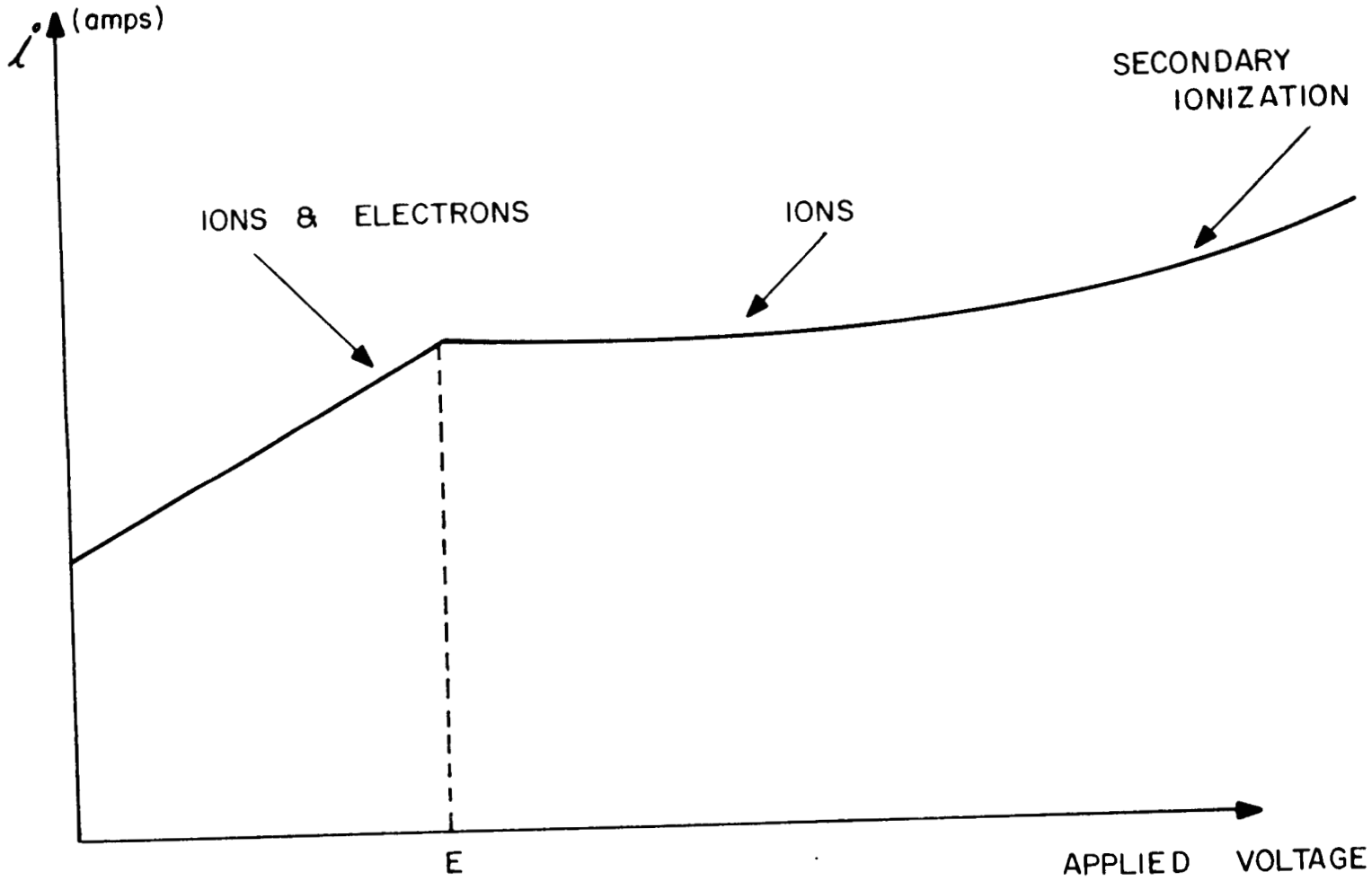

$E = h\gamma - IP$

Figure 2.

(a) high energy photons are absorbed into higher electronic states giving an excited molecule and a low energy electron, and

(b) that the released photoelectrons gain energy only to the point where they are in resonance with the many excitation levels of the molecule whereupon they excite the molecule. Both of these processes can be the source of possible fluorescence in the atmosphere.

For more detailed information on the various electron energies, a concentric cylindrical grid system has been built and is currently being tested.

The Mass Analysis of the Products of Photoionizing O_2, N_2 and CO_2 Below 1000Å (Ref. Work Statement, Item C-4)

During this Quarter, considerable progress has been achieved in this phase of the program since some support was supplied under Contract No. AF19(628)-3849. A 180-degree magnetic mass spectrometer (MS) was designed, constructed and tested. A novel feature of this MS was the employment of wedge-shaped pole pieces in order to take full advantage of the wide solid angle of focus so that a high percentage transmission (up to 50 percent) is achieved. This was particularly desirable since it is known that the photoionization efficiency is much lower than that for electron impact. Initial tests have also shown that with this MS, a 10-degree aperture can be employed and still yield a theoretical resolution of 65. For a conventional spectrometer, even an aperture of only 1 degree provides a resolution of 35. However, this high performance is not achieved without difficulty since several instrumental bugs are still present in this apparatus although for an initial model, the results appear to be extremely encouraging.

The mass analyzer was coupled to the GCA ½-meter vacuum monochromator, and the associated electronic gear and gas-filling systems were assembled and tested. The overall setup is shown schematically in Fig. 3. An appropriate light source is placed at the entrance slit so that the dispersed radiation passes through the exit slit into the reaction chamber where the absorbed radiation ionizes the sample gas. Subsequently, these photoions are accelerated and focussed onto the entrance aperture of the magnetic analyzer. The photomultiplier is employed for continuous monitoring of the dispersed photoionizing radiation, while an electron multiplier (which is not shown in the figure) is located at the collector end of the analyzer and is employed to increase the ion signal before final amplification for readout purposes.

A critical problem in the performance of these experiments is the requirement to maintain low pressures in the reaction chamber and mass analyzer without the use of optical windows (no suitable window materials exist for wavelengths below 1000Å). In this case, this is accomplished by a rather complex assembly of differential pumping. However, the detailed design characteristics of the ion chamber, reactor housing, mass analyzer, appropriate slit assemblies and differential pumping are not given in the present report. Rather, the remainder of this section is devoted to describing some laboratory results obtained by examining air samples in the present experimental setup.

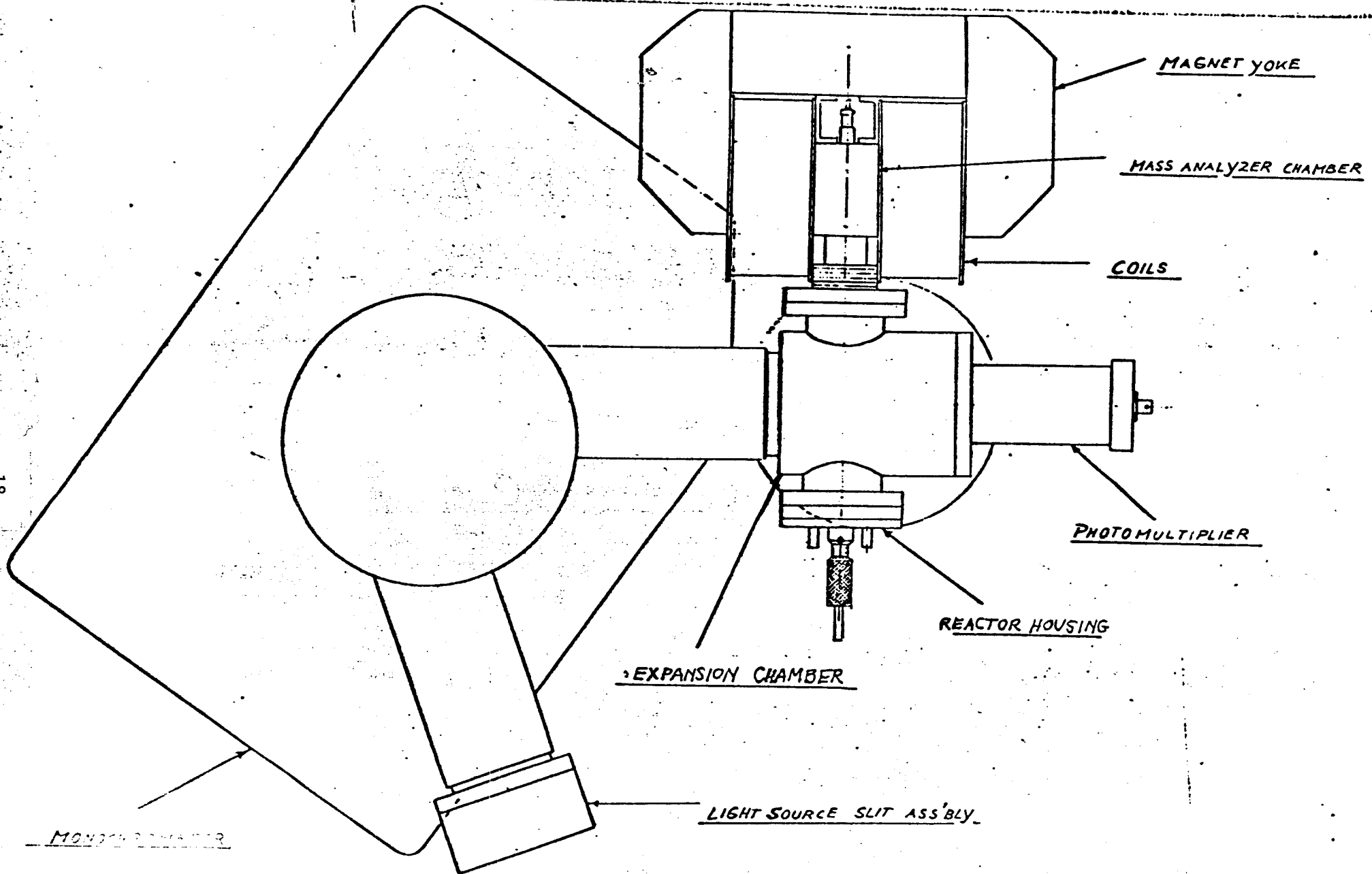
MAGNET YOKE
MASS ANALYZER CHAMBER
COILS
PHOTOMULTIPLIER
REACTOR HOUSING
EXPANSION CHAMBER
LIGHT SOURCE SLIT ASS'BLY

Figure 3.

For this purpose, a dc-operated hydrogen light source was employed to obtain radiation in the 950Å region. Since this radiation can ionize only O_2, the only ion observed was O_2^+, as expected. Figure 4 shows a plot of the ion current observed at mass number 32 as a function of pressure in the ion source. The overall behavior can probably be described as follows. The initial linear rise of the ion current is a direct consequence of the increase of light absorption according to Beer's law where for sufficiently small pressures (weak absorption), the exponential function behaves linearly. In this manner, the linear increase up to about 70 microns can be explained. At higher pressures, the full exponential law must be applied. However, it can be shown that the behavior of the data does not follow the exponential absorption law. Accordingly, a different process must be responsible for the observed behavior. In this respect, it is of interest to note that the deviations from linearity become pronounced at that pressure at which the corresponding mean free path of the gas molecules is of the same order as the dimensions of the reaction chamber. This should result in excessive scattering which will tend to broaden the ion beam so that defocussing occurs at the mass analyzer entrance slit with a corresponding loss of ion intensity. This preliminary explanation is only one of other possible explanations and the true cause of this effect must awain further investigation. In any case, it was encouraging to observe the actual generation of O_2^+ ions with 950Å radiation.

In order to check a region in which the ionization of other species occurs simultaneously, an air sample was tested at the 584Å He resonance

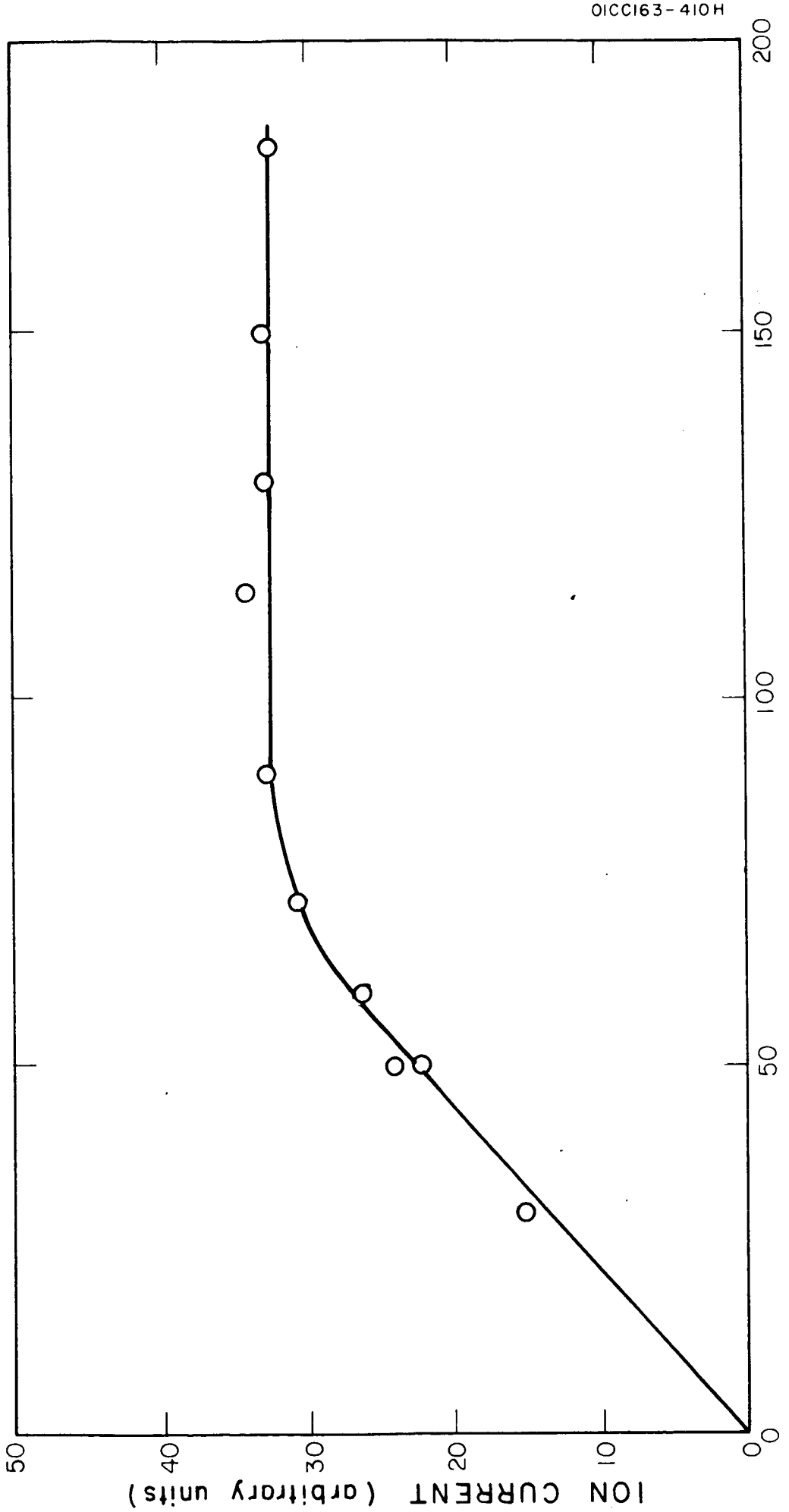
ION CURRENT (arbitrary units)
0
10
20
30
40
50
0
50
100
150
200
PRESSURE (microns)

Figure 4.

line. In this case, the primary ionic species formed by photoionization were found to be N_2^+, O_2^+ and O^+. However, here again, the observed ion intensity-pressure relationships for these ions could not be easily explained; in fact, they behaved in a more complex manner than that for the 950Å radiation.

In view of the above results, the following comments apply. It appears that on the one hand, the preliminary experimental results were very encouraging in that reliable qualitative results were obtained. However, on the other hand, the observed ion intensity-pressure characteristics indicate a behavior which is not explained in a simple manner so that the results cannot have quantitative value as yet.

D. THEORETICAL AERONOMY

There are five tasks listed in the Work Statement under theoretical aeronomy which are designated as Items D-1, D-2, D-3, D-4 and D-5. Each task is discussed in the order in which it appears in the Statement of Work.

Photoionization Rates for Constituents of the Atmospheres of Mars and Venus and CO_2 Photolysis in the Atmospheres of Mars and Venus (Ref. Work Statement, Items D-1 and D-2)

Items D-1 and D-2 are intentionally connected so that they can be discussed together. For example, under Item D-2 the CO_2 photolysis in the atmospheres of Mars has been completed by considering the following reactions:

$$CO_2 + h\nu \xrightarrow{\alpha_1} CO + O \qquad \lambda < 1750\text{Å}$$

$$CO + O \xrightarrow{k_2} CO_2$$

$$CO + O + M \xrightarrow{k_3} CO_2 + M$$

$$O + O + M \xrightarrow{k_4} O_2 + M$$

$$O_2 + h\nu \xrightarrow{\alpha_2} O + O \qquad \lambda < 2400\text{Å}$$

$$O + O_2 + M \xrightarrow{k_6} O_3 + M$$

$$O + O_3 \xrightarrow{k_7} 2O_2$$

$$O_3 + h\nu \xrightarrow{\alpha_3} O_2 + O \qquad \lambda < 3000\text{Å}$$

The parameters employed in this study reflected the latest information applicable to a study of this type. These choices are described in detail in a forthcoming GCA Technical Report. As a result of this study, the distributions have been calculated for the following species: CO_2, CO, O_2, O_3, O, N_2, and A. With proper adjustment for the diffusion of the upper atmosphere of Mars, these models could now be extrapolated for performing the required task under Item D-1; namely, to calculate the photoionization rates in the Martian atmosphere. Owing to the lack of knowledge of the major constituent, three cases are considered. First, a model is employed in which the filler gas is considered to be entirely nitrogen; another employs argon for this purpose whereas in the third case, argon and nitrogen are considered to contribute equally. It was necessary to invoke an altitude above which diffusive equilibrium obtains. This was arbitrarily chosen at that altitude where the number densities of CO and O are equal but are much greater than the local number density of CO_2. Since this region lies several kilometers above the region of maximum photochemical activity, this choice seems to be reasonable if one makes the analogy with the Earth's atmosphere in which the photodissociation of O_2 maximizes around 100 km. To illustrate the method, the model of the initial neutral particle distribution for Case (1) is shown in Figure 1. Similar models were also developed for Cases (2) and (3) but are not shown here.

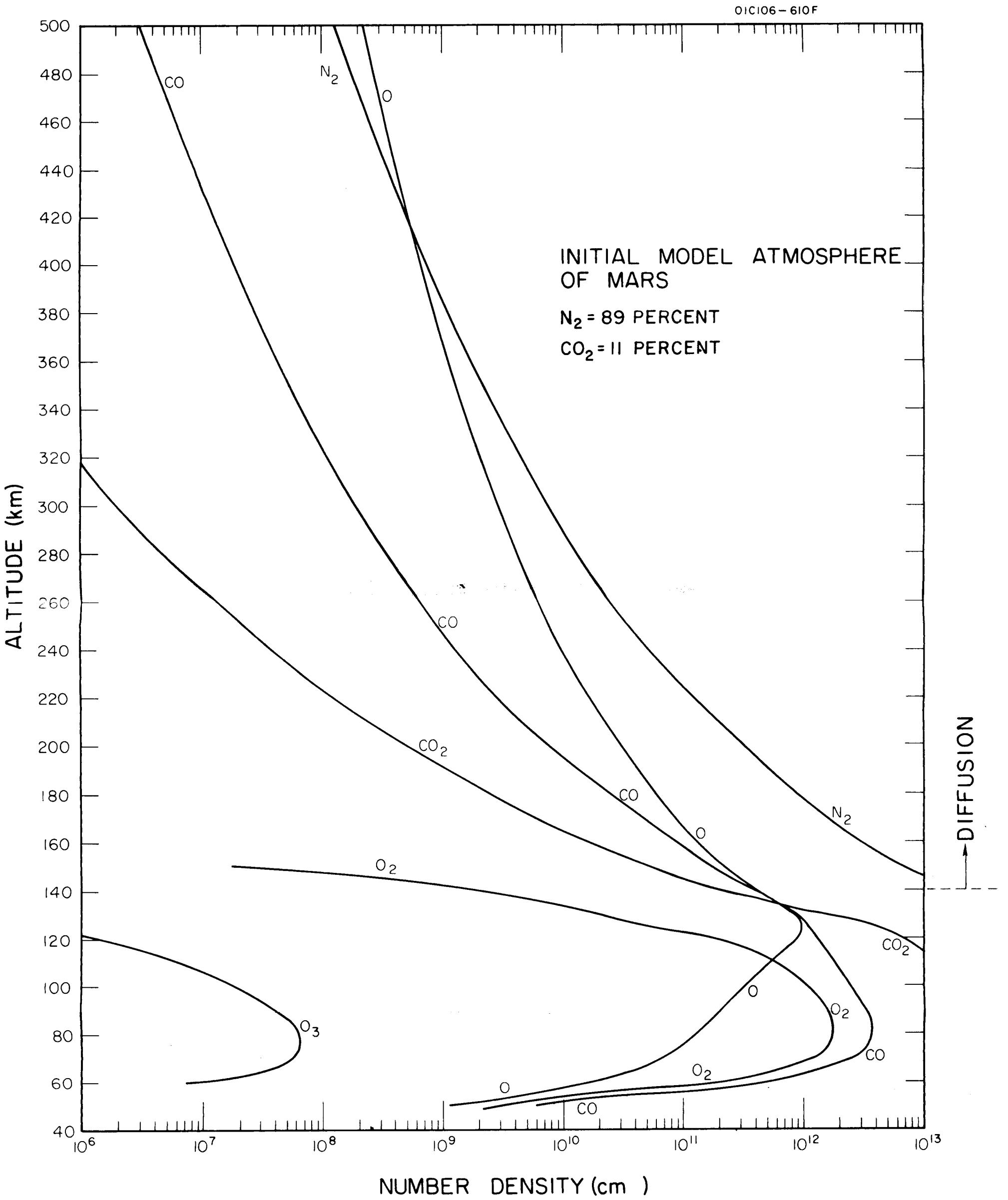
01C106-610F
INITIAL MODEL ATMOSPHERE OF MARS
N_2 = 89 PERCENT
CO_2 = 11 PERCENT
ALTITUDE (km)
NUMBER DENSITY (cm)
DIFFUSION
CO
N_2
O
CO_2
O_2
O_3
500
480
460
440
420
400
380
360
340
320
300
280
260
240
220
200
180
160
140
120
100
80
60
40
10^6
10^7
10^8
10^9
10^{10}
10^{11}
10^{12}
10^{13}

Figure 1

The indicated atmospheric models have been utilized for the calculation of the photoionization rates for the several species involved. The photoionization rate, p, in ion-pair $cm^{-3}sec^{-1}$ at a given altitude was computed according to the expression

$$p = \sum_{\lambda} I_{\lambda}(Z) \left[\Sigma \sigma_i(\lambda) n_i(Z)\right]$$

where $I_{\lambda}(Z)$ is the ultraviolet flux for a given wavelength at a given altitude, $\sigma_i(\lambda)$ is the photoionization cross section for each constituent at each wavelength, and $n_i(Z)$ is the number density of each constituent at the given altitude. These photoionization rates have been calculated for normal solar incidence and for the wavelength region $\lambda\lambda$ 900-50Å.

The required data for the solar flux, total absorption and photoionization cross sections were extracted from the several GCA Technical Reports generated under the present program for this express purpose. The computed photoionization rates are shown in Figures 2, 3, and 4 for the three initial model atmospheres. The dotted lines represent the photoionization rates for the individual species whereas the total ionization rates are shown by solid lines.

It is planned to perform similar calculations for the planet Venus as soon as the CO_2 photolysis studies have been accomplished. The resulting models will probably not be as physically acceptable as

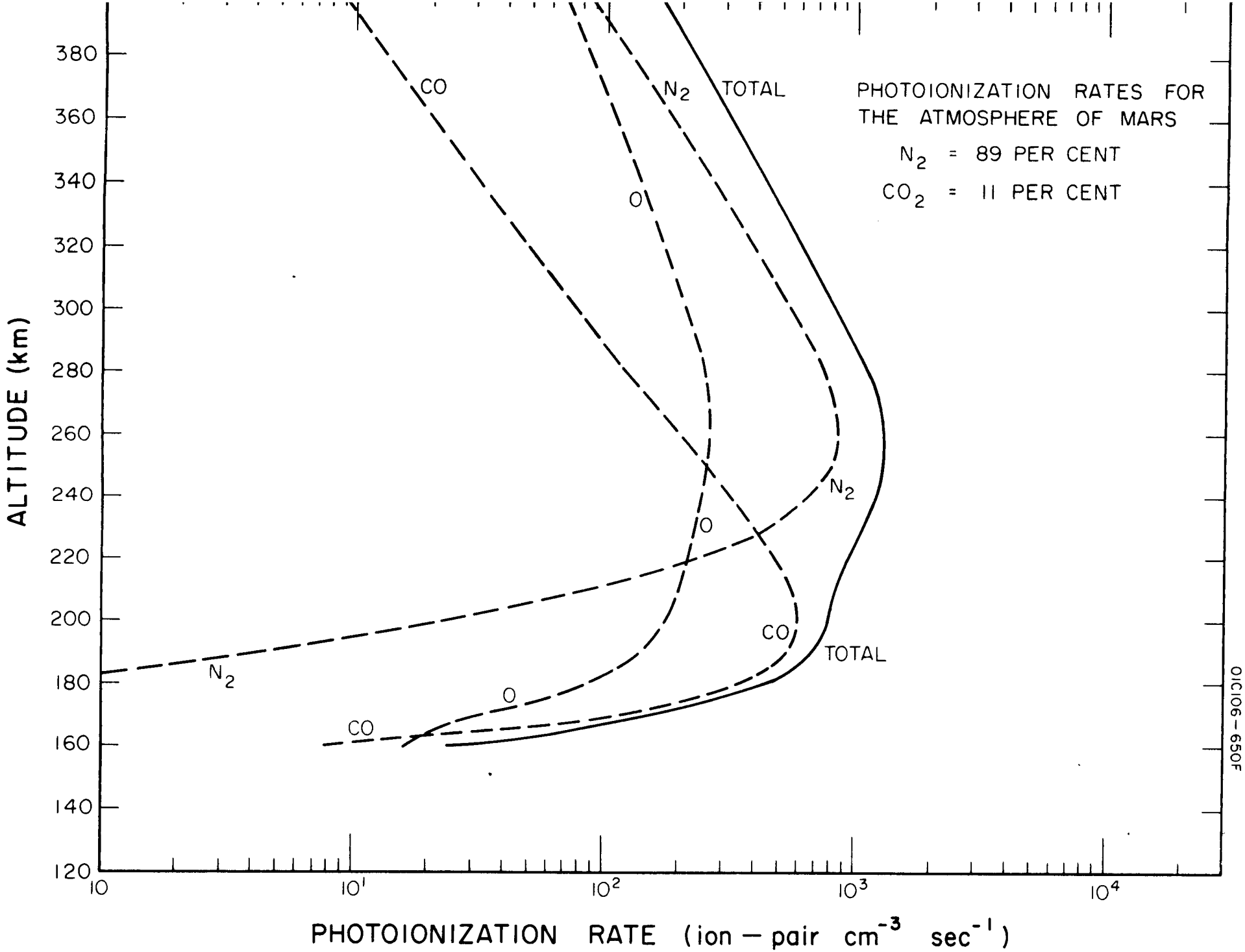
PHOTOIONIZATION RATES FOR
THE ATMOSPHERE OF MARS
N_2 = 89 PER CENT
CO_2 = 11 PER CENT
CO
N_2
TOTAL
O
N_2
O
CO
TOTAL
N_2
O
CO
ALTITUDE (km)
380
360
340
320
300
280
260
240
220
200
180
160
140
120
10
10^1
10^2
10^3
10^4
PHOTOIONIZATION RATE (ion − pair cm^{-3} sec^{-1})
01C106-650F

Figure 2

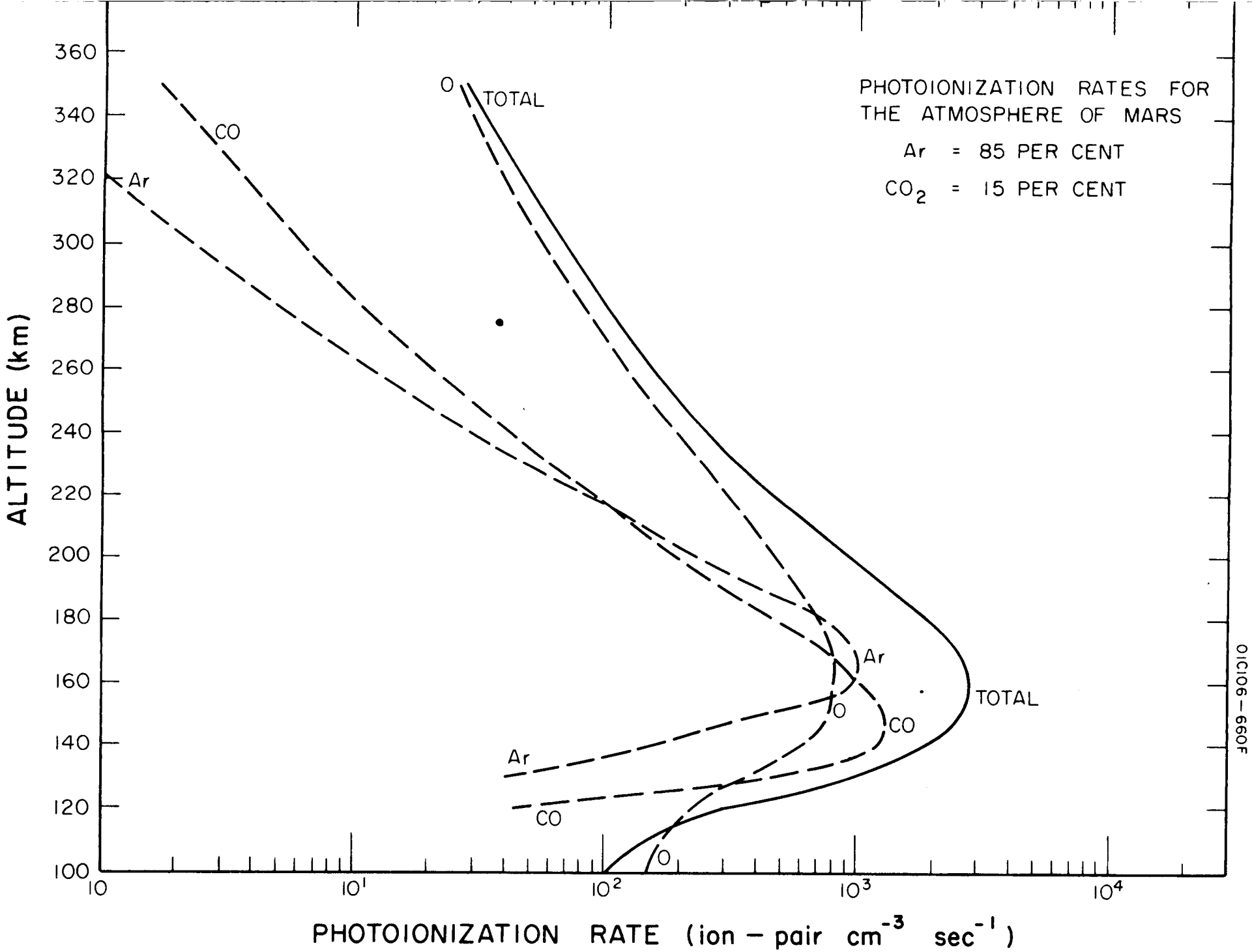
PHOTOIONIZATION RATES FOR
THE ATMOSPHERE OF MARS
Ar = 85 PER CENT
CO_2 = 15 PER CENT
ALTITUDE (km)
PHOTOIONIZATION RATE (ion − pair cm^{-3} sec^{-1})
TOTAL
CO
Ar
O
360
340
320
300
280
260
240
220
200
180
160
140
120
100
10
10^1
10^2
10^3
10^4
0101O6—660F

Figure 3

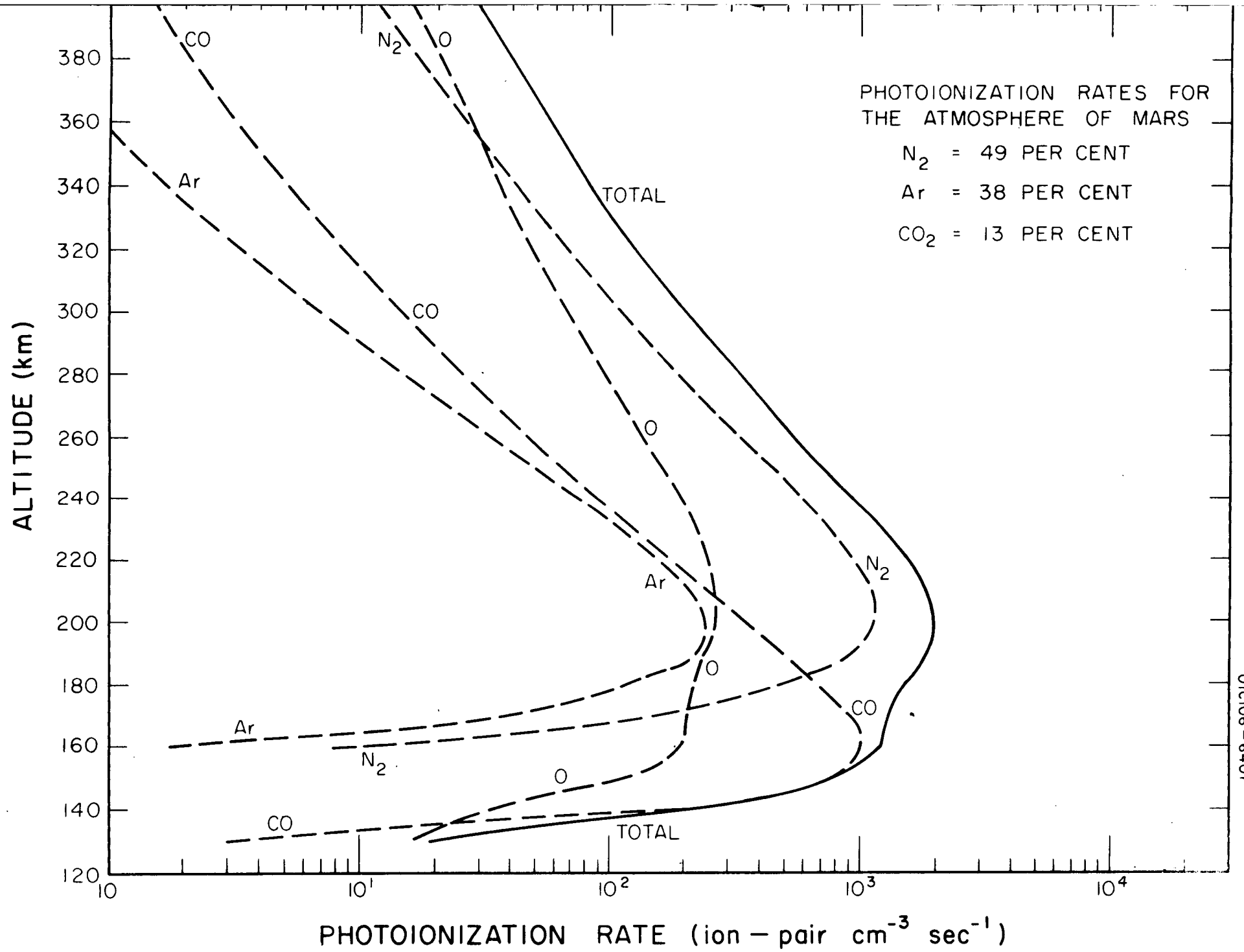
PHOTOIONIZATION RATES FOR
THE ATMOSPHERE OF MARS
N_2 = 49 PER CENT
Ar = 38 PER CENT
CO_2 = 13 PER CENT
ALTITUDE (km)
PHOTOIONIZATION RATE (ion − pair cm^{-3} sec^{-1})
CO
N_2
O
Ar
TOTAL
380
360
340
320
300
280
260
240
220
200
180
160
140
120
10
10^1
10^2
10^3
10^4
01C106-640F

Figure 4

those for Mars due to our lack of knowledge concerning Venus. In any case, the calculations will be performed and submitted before the termination of the present contract.

The Role of Cosmic Dust Deposited in the Upper Atmospheres of Earth, Mars and Venus (Ref. Work Statement, Item D-3)

In the last Quarterly Report, new source functions were described together with a usable profile for the diffusion coefficient with altitude. These improved parameters are now being employed to obtain a more physically acceptable model for the debris deposition in the Earth atmosphere. It is hoped that there will be enough time to compare these findings with the recent mass spectrometric experimental discovery of ions of sodium, magnesium and calcium in an attempt to correlate their source to interplanetary debris.

The Intensity of N_2^+, O_2^+ and O^+ Visible Radiation Arising from Fluorescence of the Solar Ultraviolet (Ref. Work Statement, Item D-4)

This theoretical study is proceeding on schedule so that it is anticipated that it should be completed before the termination of the present contract. It is presently planned to report the findings of this work in the next Quarter.

Quantum Calculations on the Transition Probabilities of Lines of O, N, O^+ and N^+ (Ref. Work Statement, Item D-5)

This phase of the work has been completed and is described in detail in the following publications:

(a) "An Expansion Method for Calculating Atomic Properties - I. The ^2S and $^2P^o$ States of the Lithium Sequence" [M. Cohen and A. Dalgarno, GCA Technical Report No. 64-5-N].

(b) "An Expansion Method for Calculating Atomic Properties - II. Transition Probabilities" [M. Cohen and A. Dalgarno, GCA Technical Report No. 64-6-N and Proc. Roy. Soc. A280, 258, 1964].

E. LUMINOSITY OF PLANETARY GASES

There are seven tasks listed in the Work Statement under luminosity of planetary gases which are designated as Items E-1, E-2, E-3, E-4, E-5, E-6 and E-7. Each task is discussed in the order in which it appears in the Statement of Work.

The Measurement of the Rayleigh Defect Below 2000Å and the Measurement of Scattering Cross Sections at Lyman-Alpha and Other Wavelengths for the Rare Gases, Molecular Hydrogen and Nitrogen (Ref. Work Statement, Items E-1 and E-2).

During this Quarter the experimental portion of Items E-1 and E-2 of the program has been completed since measurements have been obtained for the relative scattering cross sections at 1215.6Å for helium, neon, argon, hydrogen and nitrogen. The experimental setup consisted of a microwave-powered hydrogen light source with an oxygen filter to isolate Lyman-alpha. The intensity of the incident radiation was monitored by a photon counter (a gas ionization chamber) whereas the scattered radiation was measured by a vacuum uv sensitive Geiger counter. The results are compared to some recent theoretical values due to Dalgarno (private communication).

The details will be included in a forthcoming GCA Technical Report on this specific work; however, a brief description of the investigation is given below.

The over-all experimental setup is schematically shown in Figure 1 where the appropriate letters are defined as follows:

B	Baffle	Mc	McLeod Gauge
CT	Cold Trap	NV	Needle valve
CTC	Cold Trap(copper turnings)	OM	Oil manometer
D	Diffusion pump	SGT	Silica-gel trap
FM	Flow meter	T	Gas-tank
FP	Fore-pump	Th	Thermocouple gauge
GD	Glass diffusion pump	VG	Vacuum Gauge
DF	Glass filter	R	Reservoir
GV	Gate Valve	Z	Zeolite or charcoal trap
Hg	Mercury gauge		

The gas was introduced into the system through a needle valve and then purified by passing through P_2O_5, a silica-gel trap, a Zeolite trap, a fine porosity glass filter, and finally a cold trap packed with corrugated copper turnings. When hydrogen, neon or helium was employed, the charcoal trap was cooled by liquid nitrogen. For argon and nitrogen, the Zeolite trap was cooled by dry-ice slush. Pressures of the gas were measured mainly by mercury manometers (MN 1100 Gauge, Manostat Corp.), and the values were corrected to the values at 25°C. Other vacuum gauges were also employed for subsidiary purposes.

The basic design of the albedo chamber is illustrated in Figure 2. The incident light from the light source S is collimated by C and was continuously monitored by measuring the reflected light from the small mirror at M by means of a photoionization counter at D. The scattered light at the observation area A is measured at right angle to the incident light by the calibrated Geiger counter.

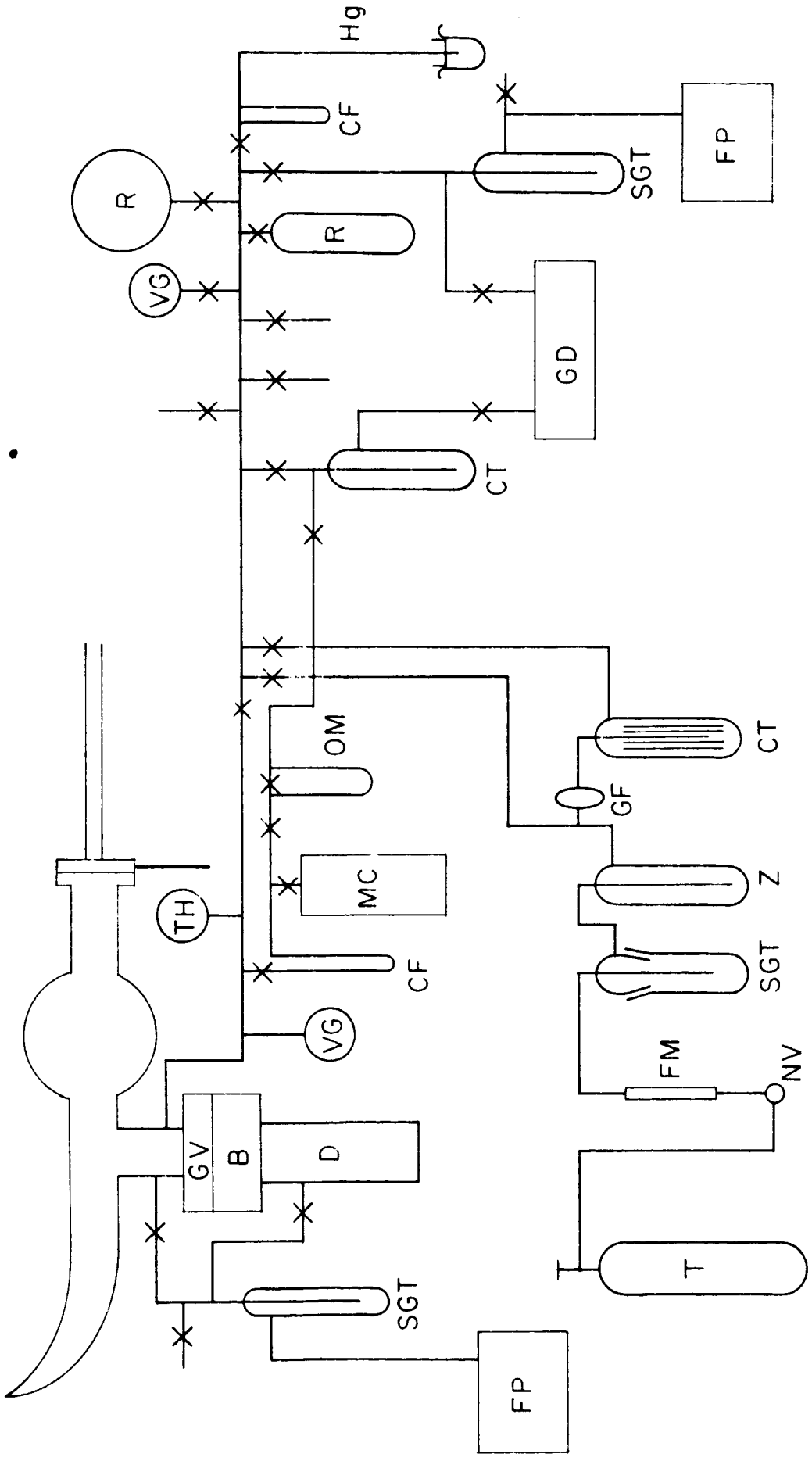

Figure 1.

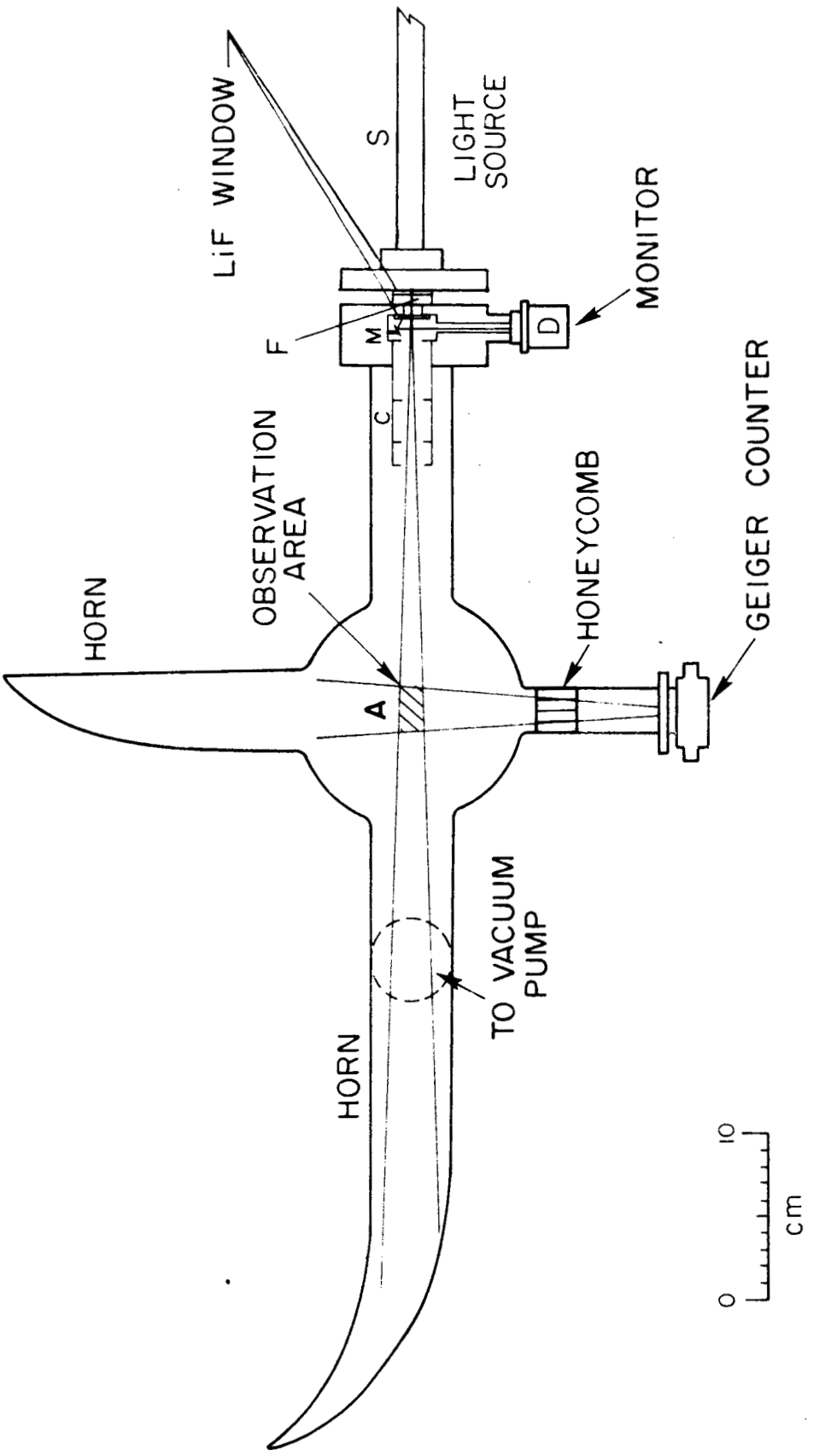
LiF WINDOW
S
LIGHT SOURCE
MONITOR
F
M
D
C
OBSERVATION AREA
HONEYCOMB
GEIGER COUNTER
HORN
A
TO VACUUM PUMP
HORN
0
10
cm

Figure 2.

Another feature of the apparatus is the installation of an oxygen filter, F, for spectral isolation of the Lyman-alpha radiation. This feature was verified by independent measurements performed with a 2-meter uv monochromator which indicated that the filter definitely restricts the radiation to Lyman-alpha.

Briefly, the following experimental procedure was used. Prior to experimentation, the electronic components were allowed to reach a stationary state. Then, the hydrogen lamp output was adjusted to 1×10^{-10} amps by adjusting the power of the microwave generator. The flow rate and the pressure of the gas in the hydrogen lamp, the pressure of oxygen in the oxygen filter and all other conditions were set at specific pre-fixed values. The high voltage to the counter was adjusted so that a pulse height corresponding to 1.5 volts was observed on the oscilloscope since independent experimentation indicated that this was an optimum voltage for operating in the "flat" region of the calibration curve.

First the background count was noted (usually less than 5 c/sec). Then the appropriate gas was admitted into the albedo chamber and the scattered intensity was measured as a function of sample gas pressure. Through all the measurements, the incident light was monitored continuously and was adjusted to remain constant; the pulse height of the Geiger counter was adjusted to the same value. The time constant of the count rate meter was chosen at proper values for each counting rate in the range of 40 sec to 80 sec so that a smooth recorder curve was obtained.

Each measurement was recorded only after a constant count was observed for at least five consecutive minutes. Corrections due to the error of the count rate meter and also those due to the dead time of the Geiger counter were applied to the observed values. The temperature of the gas in the chamber was recorded so that the pressures measured by the manometer could be normalized to a temperature of 25°C.

Classical electromagnetic theory shows that a linear relationship holds between the intensity of the unpolarized incident light and the number of photons, scattered per solid angle to the incident beam. Accordingly, the relative scattering cross section can be experimentally determined from plotting count number against the pressure of the sample gas and relating the slope of the line (which should be a straight line) to the scattering cross section of the gas.

The corrected values of the observed count rates were plotted against pressure and it was noted that in each case the resulting graphs exhibited good linearity as evident in Figures 3, 4, 5, 6, and 7. From the slopes of the graphs, the relative scattering cross sections were computed; the values are given in Table I which, for ready comparison, includes some recent theoretical calculations due to Dalgarno (private communication). Excellent agreement is indicated for the rare gases

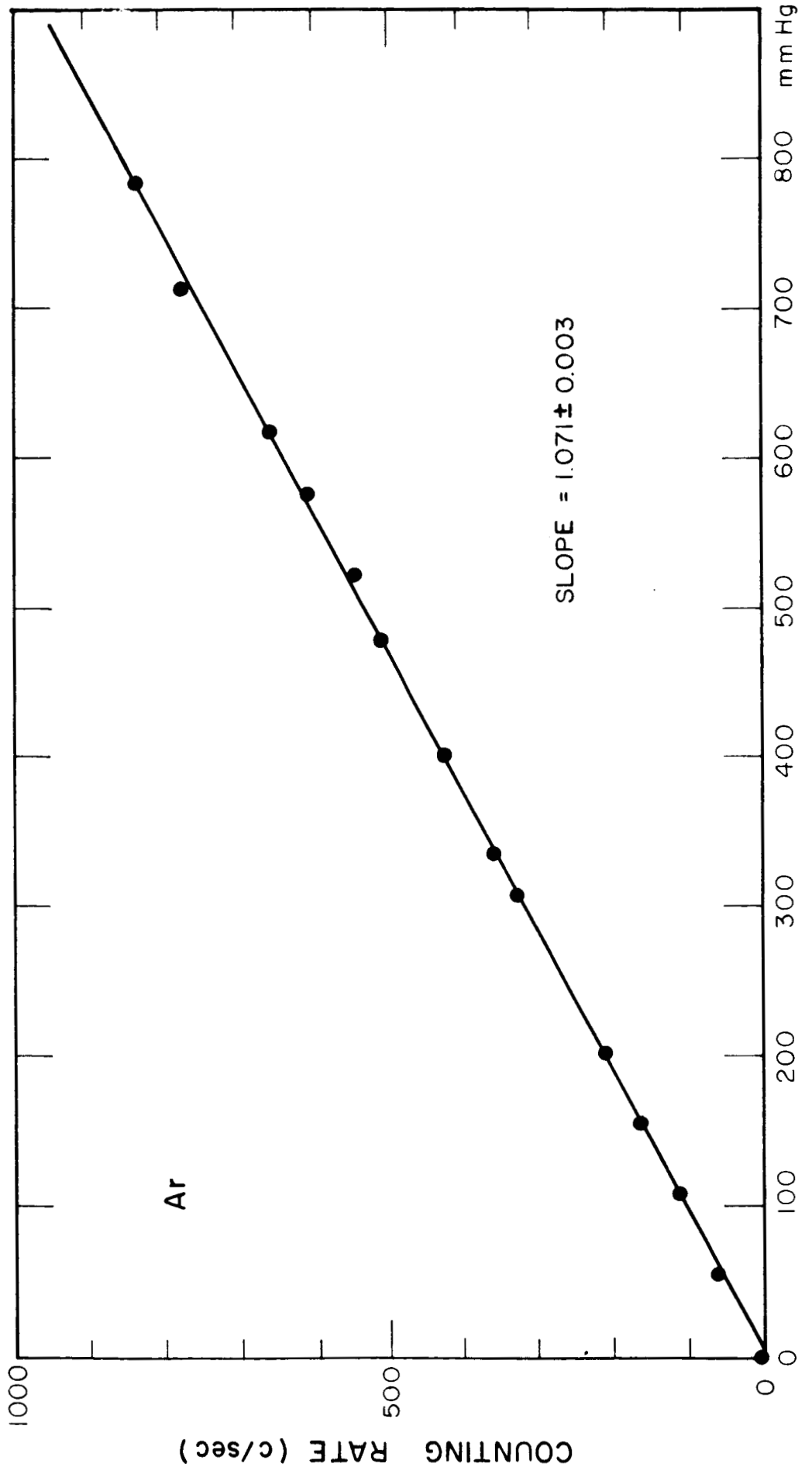
COUNTING RATE (c/sec)
1000
500
0
Ar
SLOPE = 1.071 ± 0.003
0
100
200
300
400
500
600
700
800
mm Hg
PRESSURE OF ARGON

Figure 3.

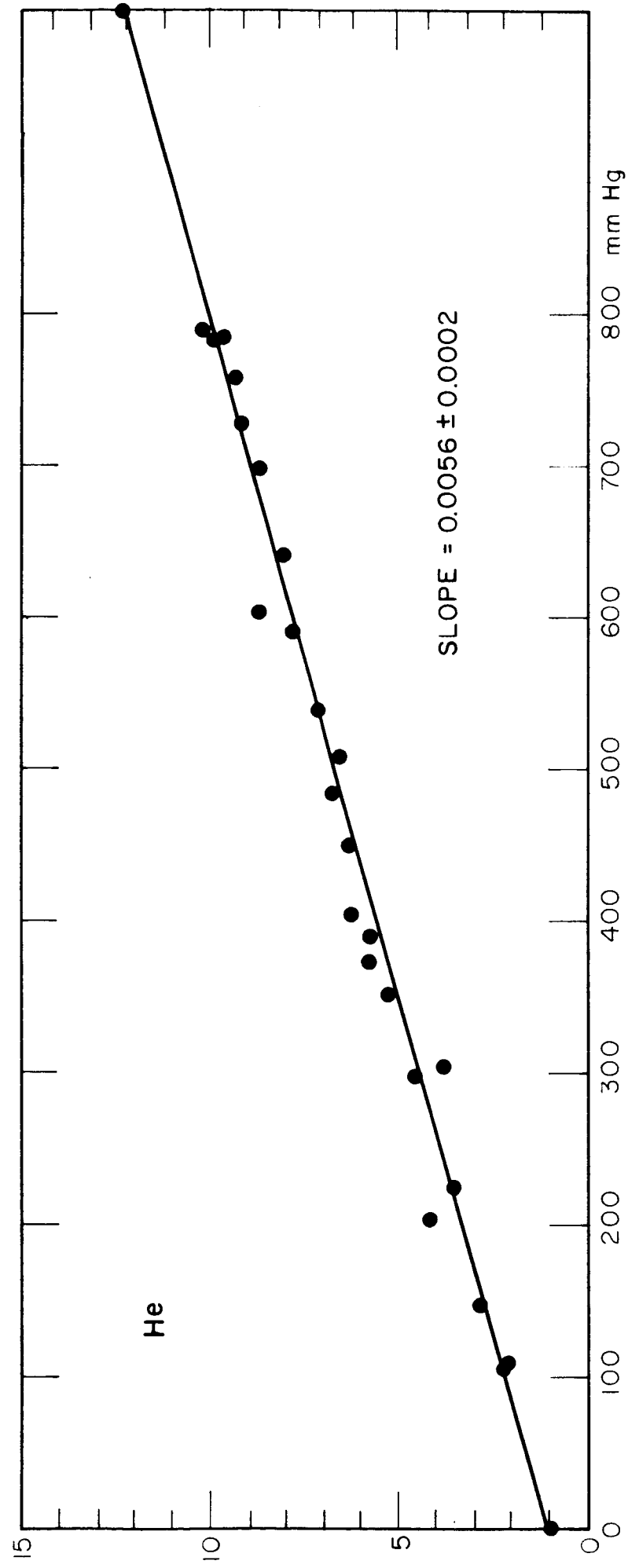
He
SLOPE = 0.0056 ± 0.0002
COUNTING RATE (c/sec)
PRESSURE OF HELIUM
mm Hg
0
5
10
15
100
200
300
400
500
600
700
800

Figure 4.

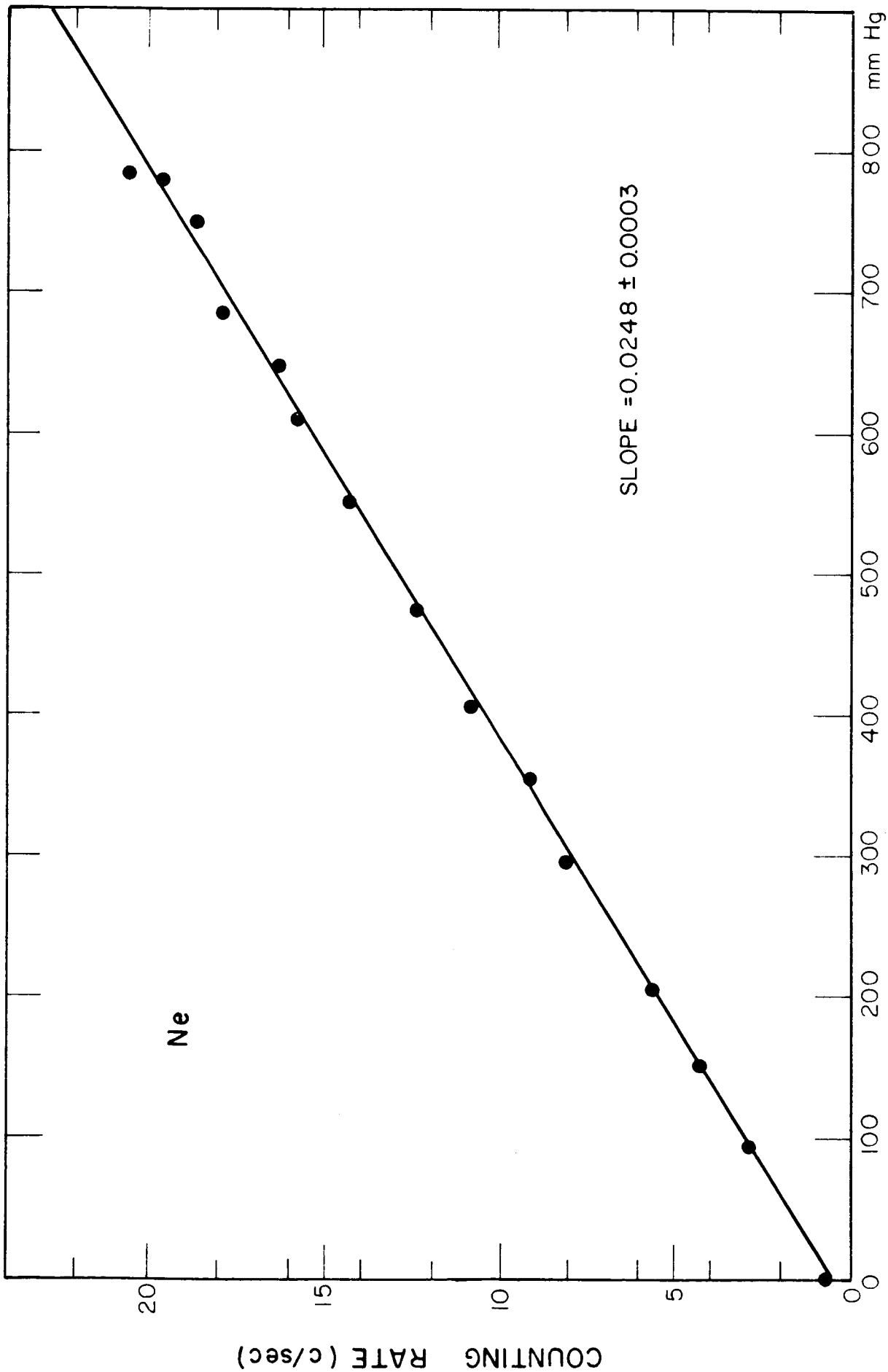
Ne
SLOPE =0.0248 ± 0.0003
COUNTING RATE (c/sec)
0
5
10
15
20
PRESSURE OF NEON
0
100
200
300
400
500
600
700
800
mm Hg

Figure 5.

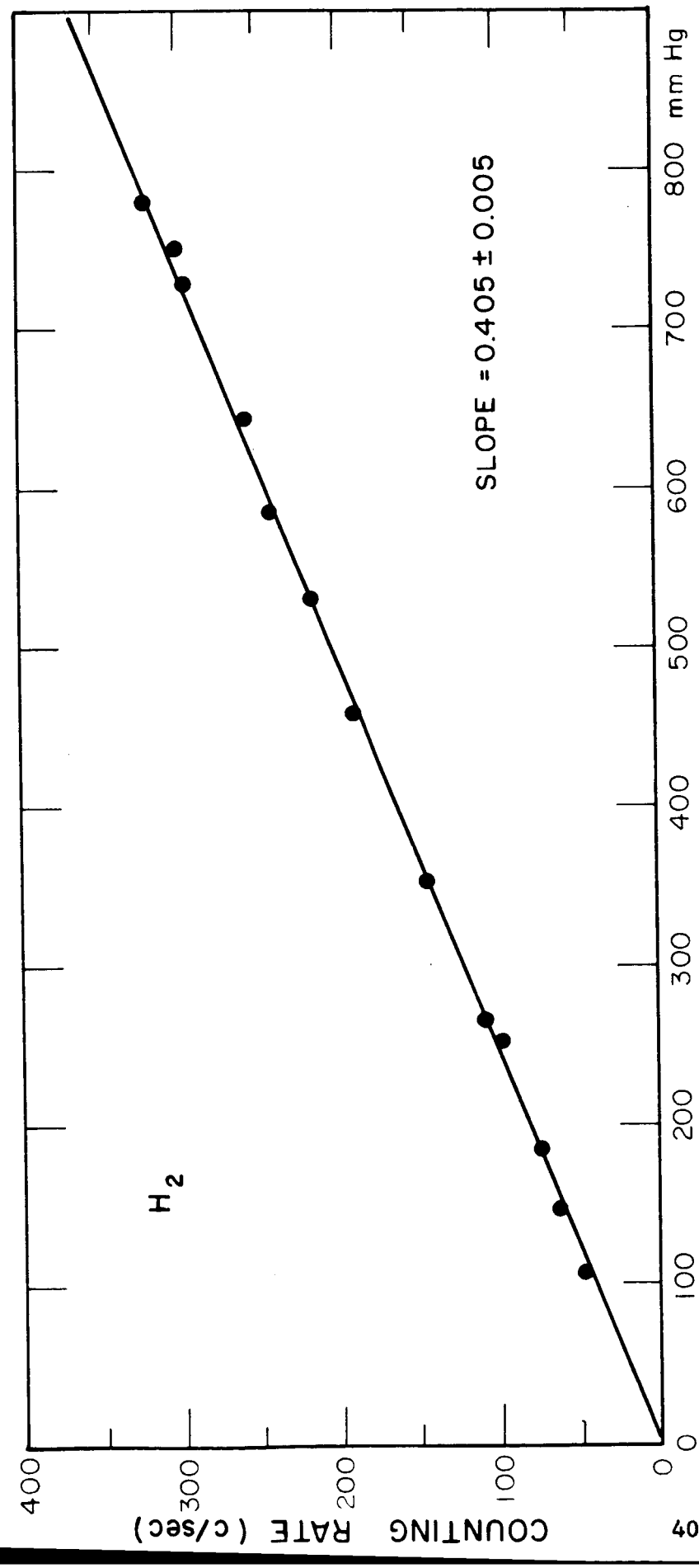
400
300
200
100
0
COUNTING RATE (c/sec)
40
0
100
200
300
400
500
600
700
800 mm Hg
PRESSURE OF HYDROGEN
SLOPE = 0.405 ± 0.005
H_2

Figure 6.

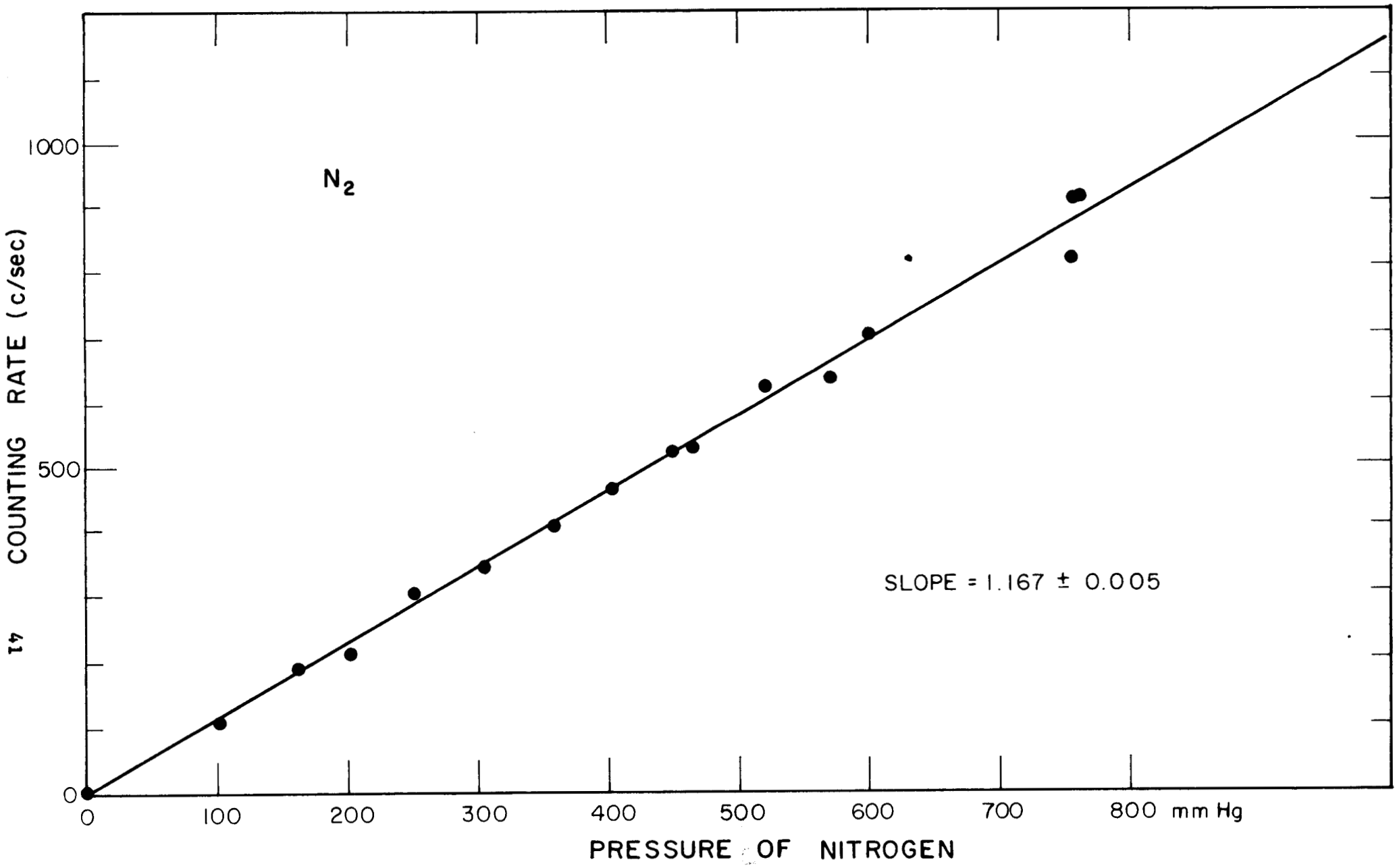

Figure 7.

TABLE I.

SCATTERING CROSS SECTIONS* AT LYMAN-ALPHA FOR SEVERAL GASES

	EXPERIMENTAL		THEORETICAL
	Normalized Vs. Argon	Normalized Vs. Helium	After A.Dalgarno**
A	63	67	63
He	.33	.35	.35
Neon	1.4	1.5	1.4
H_2	23	25	18
N_2	67	72	---
Krypton	---		
Xenon	---		

* All values to be multiplied by 10^{-25} cm^2.

** Private Communication.

which can be handled on a theoretical basis. The "disagreement" with the bimolecular cases is not surprising and probably reflects the limitations of present theoretical techniques when employed for molecules. In any case, a more detailed comparison is given in a forthcoming GCA Technical Report.

Fluorescence Radiation of O_2, N_2 and CO_2 (Ref. Work Statement, Item E-3).

When photoelectrons are released with energies $\geq$ to the energy of a resonance level in an atom, there is a high probability that resonance radiation will be excited. This will be possible only at photon energies $h\nu$ such that

$$h\nu \geq IP(X) + X^* ,$$

where $IP(X)$ is the ionization potential and X^* the excitation energy of the atom. For helium this takes place for $\lambda \geq 271\text{Å}$ and for argon at $\lambda \geq 450\text{Å}$. By measuring the photoelectron energies in helium we have observed a sudden loss of high energy electrons at wavelengths below 270Å indicating that their energies have been lost in excitational collisions with neutral helium. This is indirect evidence for the production of 584Å fluorescence in helium at wavelengths below 270Å. No experimental attempt has been accomplished as yet to observe this expected radiation.

Measurement of Scattering Cross Sections in the Vicinity of Resonance Lines (Ref. Work Statement, Item E-4).

The measurement of scattering cross sections in the vicinity of resonance lines can be accomplished by the employment of a monochromator. Two methods present themselves; the first in which the albedo chamber described previously is attached to the monochromator and/or second, an attenuation method is employed in which a high pressure cell is attached to the exit slit of the monochromator to observe the "attenuation" due to the scattering cross section.

The salient features of the first technique are shown in Figure 8. It may be noted that the look angle is taken as $54^{\circ}43'$ since it can be theoretically demonstrated that this signal would be essentially three times more intense than that at right angles. Moreover, the observed intensities at this angle do not depend on the degree of depolarization. The critical factor for the performance of this experiment is the intensity of the scattered radiation. It can be expected to be down by 4 to 5 orders of magnitude when compared to the previously-described scattering experiments which used undispersed radiation. On the other hand, the background should be correspondingly smaller so that the question of feasibility of this technique is still open. It may be noted that the technique is applicable only to those gases which have a relatively low scattering cross section. For the measurement of gases of high scattering cross sections, an attenuation technique must be employed as described below.

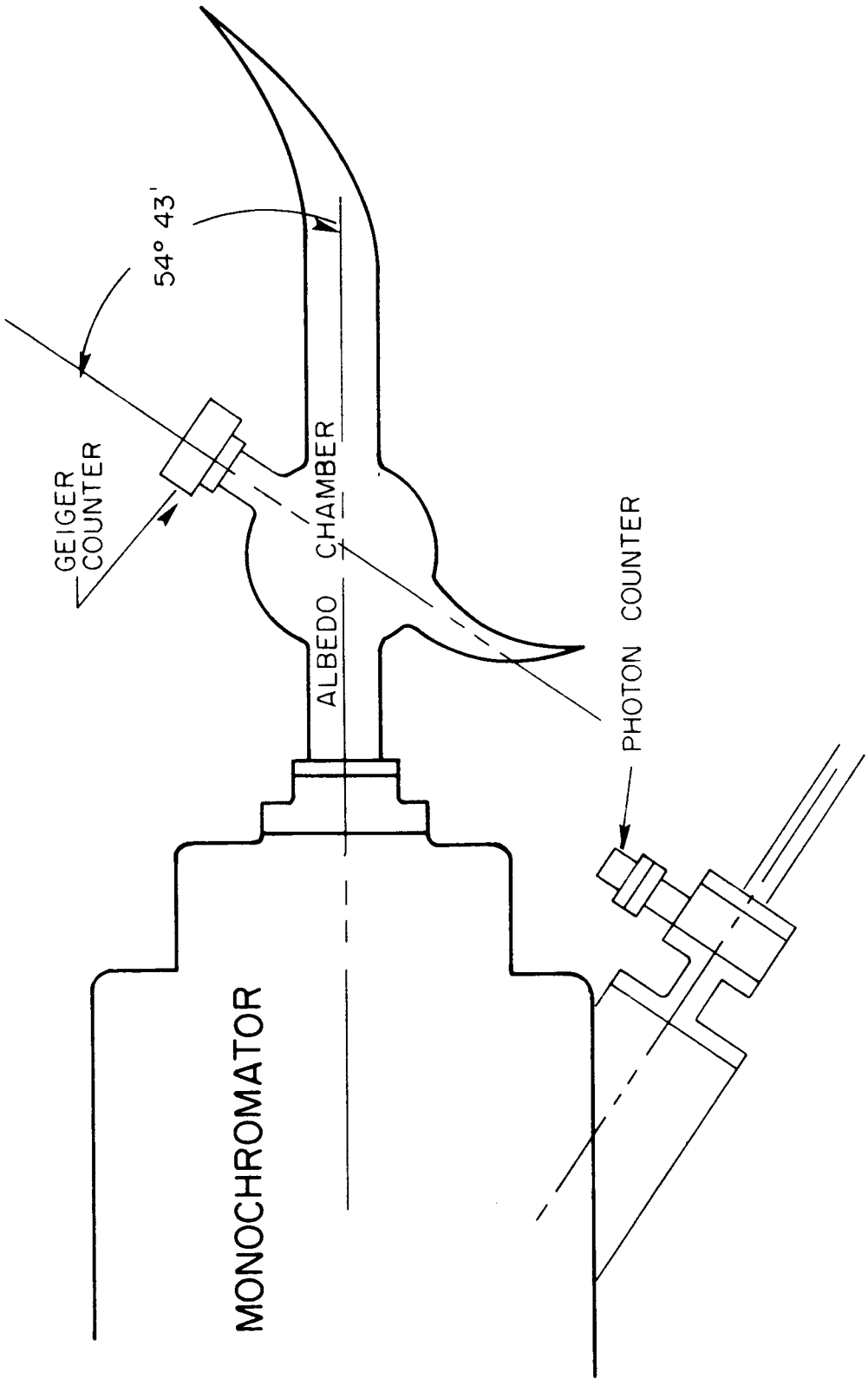
54° 43'
GEIGER COUNTER
ALBEDO CHAMBER
PHOTON COUNTER
MONOCHROMATOR

Figure 8

The features of the attenuation technique are illustrated in Figure 9. It is clear from this schematic that this technique is rather straightforward and avoids many of the severe difficulties encountered in the direct scattering method. For example, in this method, essentially the same techniques are involved as those employed for ordinary absorption measurements.

The appropriate apparatus for both methods have been designed and constructed during this Quarter. It may be pointed out here that in both of these methods, the scattering efficiency as a function of wavelength can be obtained by scanning through the appropriate spectral region with the monochromator, this is in essence the present plan for obtaining the later required under this phase of the program.

Spectral Reflectivity and Luminosity of the Atmospheres of Mars, Earth and Venus (50Å Bandwidths for the Region Below 2000Å (Ref. Work Statement, Items E-5, E-6 and E-7).

The spectral reflectivity and luminosity of the atmospheres of Mars and Earth have been completed for 50Å bandwidths for the region below 2000Å (see QPR No.3). Although it was planned to calculate these data for 1Å resolution as an additional task not required under the present contract, it turns out that the remaining funds can be utilized better for the performance of the remaining required tasks. In the last Quarterly, it was pointed out that a suitable model for the upper atmosphere of Venus was derived in spite of the fact that the data are sparse. During the coming Quarter, it is expected to apply this model

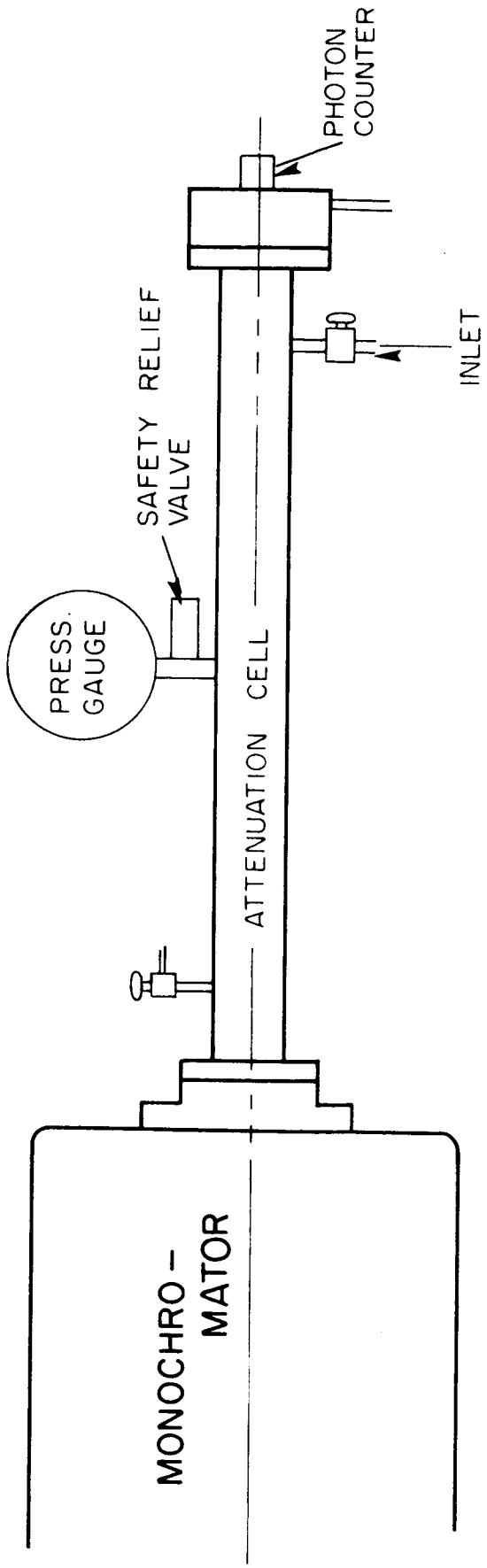
PHOTON COUNTER
INLET
SAFETY RELIEF VALVE
PRESS. GAUGE
ATTENUATION CELL
MONOCHRO – MATOR

Figure 9

to perform the required calculations so that it can be anticipated that the 50Å bandwidth reflectivity and luminosity calculations will be completed for Mars, Earth and Venus before the termination of the present contract. Finally, some effort is currently being directed towards examining the role of airglow, chemiluminescence, fluorescence and resonance radiation in planetary atmospheres.

III. ADDITIONAL WORK

During this Quarter a paper entitled "On the Ozone Distribution in the Atmosphere of Mars" by F. F. Marmo, ShardaNand and P. Warneck was submitted to the Journal of Geophysical Research for publications. It is reproduced here in its entirety.

Ozone formation in the lower atmosphere of Mars via the solar photolysis of oxygen has been previously investigated by Marmo and Warneck (1961) who found the resulting steady state ozone concentration to increase monotonically with decreasing altitude with the maximum ozone concentration occurring at the surface of the planet. However, a more recent study by Paetzold (1963) took exception to this view, since it suggested the existence of an ozone concentration peak at an altitude of around 40 km. From his results Paetzold derived conclusions concerning the stratospheric circulation and wind patterns, which can serve to demonstrate the importance of the Martian ozone distribution profile. The present note, accordingly, is concerned with the conflict between the previous notions about the ozone distribution profile and those advanced by Paetzold's paper.

There is agreement that the basic photochemical reactions involved in the atmosphere of Mars are:

$$(1)\quad O_2 + h\nu \longrightarrow O + O \qquad \lambda \leq 2400\text{Å}$$

$$(2)\quad O + O_2 + M \longrightarrow O_3 + M \qquad k_2$$

(3) $O + O_3 \longrightarrow O_2 + O_2$ k_3

(4) $O_3 + h\nu \longrightarrow O_2 + O$ $\lambda \leq 3000\text{Å}$

(5) $O + O + M \longrightarrow O_2 + M$ k_5

(6) $CO_2 + h\nu \longrightarrow CO + O$ $\lambda \leq 1750\text{Å}$

(7) $CO + O \longrightarrow CO_2$ k_7

At altitudes below about 80 km a significant photodissociation of CO_2 can be precluded owing to the opacity of the Martian atmosphere for wavelengths below 1750Å, so that reactions (6) and (7) can be ignored (Marmo and Warneck 1961; Paetzold 1963; Schimizu 1963). Paetzold obtained the 40 km ozone concentration peak by applying only reactions (1) through (4); he also assumed a temperature distribution with a lapse rate of 2.5 degrees/km and a tropopause at 40 km. Marmo and Warneck, on the other hand, assumed an isothermal atmosphere but used reactions (1) through (5). The discrepancy between the two sets of results must obviously be attributed either to the difference in the temperature profiles, or to the inclusion of reaction (5) in the set of reactions applied. The temperature variation mainly affects reaction (3), since the other reactions are roughly independent on temperature (Kaufman 1963). The influence of the temperature profile and that of reaction (5) were examined in the present calculations which make use of the previously-described iteration procedure to obtain self-consistent steady-state distributions of ozone (Marmo and Warneck 1961). The basic data summarized in Table 1 were employed.

TABLE 1

Parameters Used and Their Source

Surface temperature 250°K Lapse rate 2.9 degree/km Tropopause at 30 km altitude	Schilling (1963)
Surface pressure 25 mbar Constituents: 470 meters NTP N_2: 55 meters NTP CO_2; 70 cm NTP O_2.	Kaplan, Munch and Spinrad (1964)
Solar flux on top of Earth atmosphere in 50Å intervals 1750-3000Å wavelength region	Detwiler, Garret, Purcell and Tousey (1961); Johnson (1954)
Average dilution factor to account for diminution of solar flux in the vicinity of Mars $\mu = 0.444$	
Absorption cross sections for oxygen and ozone 1750-3000Å wavelength region	Gast (1961) Inn and Tanaka (1953); Watanabe, Zelikoff and Inn (1953)
Photodissociation yield factors for oxygen and ozone: assumed to be unity.	
Rate constants: $k_2 = 2.2 \times 10^{-34}$ cc^2/molec^{2}sec $k_3 = 5 \times 10^{-11}$ exp(-6000/RT)cc/molec sec $k_5 = 2.8 \times 10^{-33}$ cc^2/molec^{2}sec.	Kaufman (1963)

In Figure 1 are shown the ozone distributions obtained (a) from an application of the four reaction systems used by Paetzold; and (b) when reaction (5) is included in the mechanism. It is evident that the use of reactions (1) through (4) produces an ozone peak at the tropopause level, whereas if (5) is included, the set of reactions yields an ozone profile which is in essential agreement with the results derived earlier by Marmo and Warneck (1961). This shows that reaction (5) is the overriding factor and that the temperature effect associated with (3) is negligible.

Some further calculations were performed in order that the influence of other parameters could be obtained. The effect of lowering the surface pressure to 10 mbar, keeping the oxygen content constant at the same time, was to decrease the ozone concentrations by a factor of about two, while the shape of the distribution remained essentially unaltered. When the nitrogen content was replaced by the same amount of argon, the change in the total ozone concentration was found to be negligible, but the ozone concentration decreased more rapidly with altitude. This latter effect is mainly due to the difference in molecular weight of the bulk of the atmosphere which affects the scale height. None of these parameter variations, however, resulted in the development of an ozone layer.

Finally, a lowering of the oxygen content decreased the total amount of ozone by approximately the same factor (this is in agreement with both Marmo and Warneck 1961 and with Paetzold 1963) without appreciably affecting the ozone distribution. Conversely, even for an oxygen

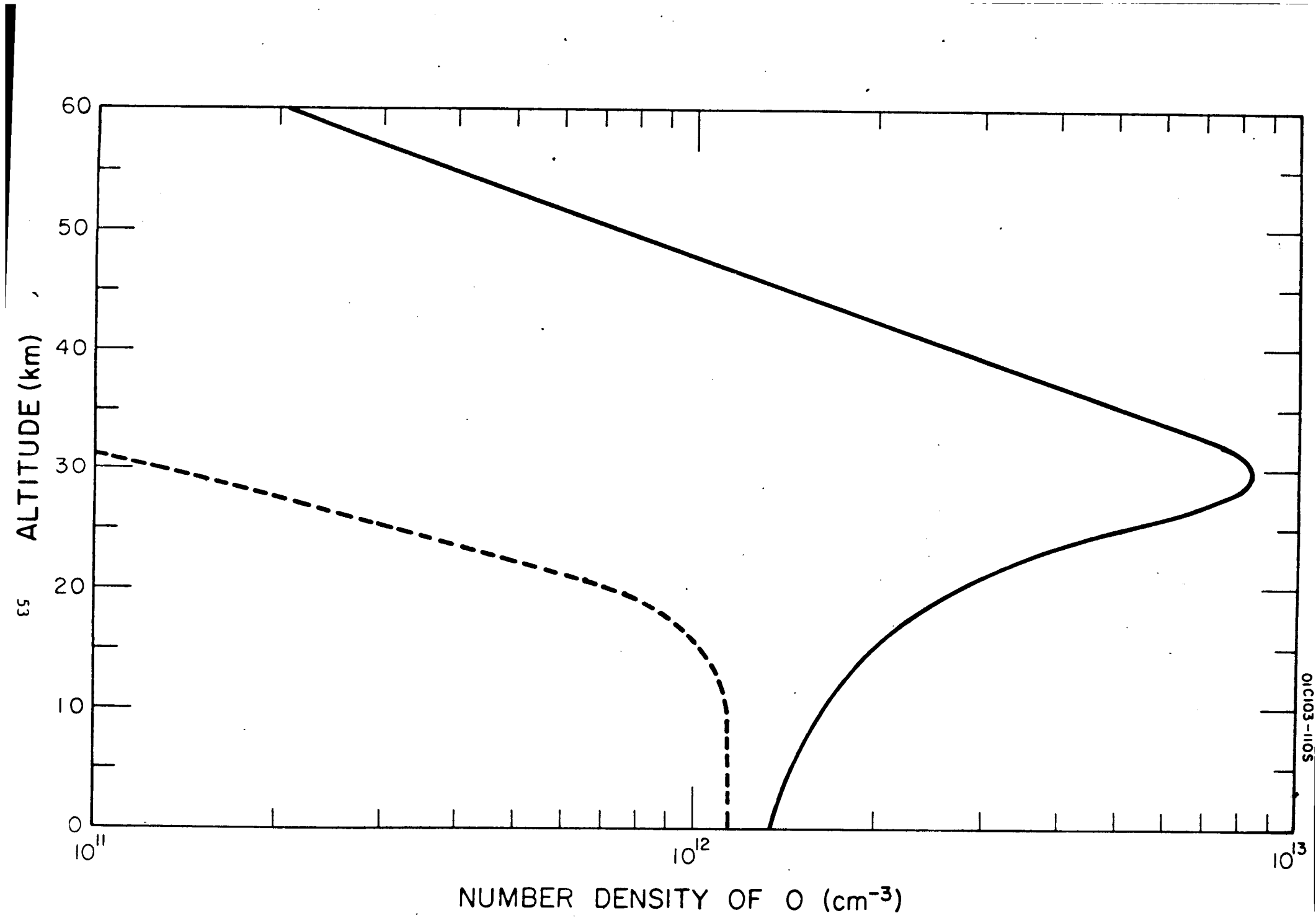
60
50
40
30
20
10
0
ALTITUDE (km)
10^{11}
10^{12}
10^{13}
NUMBER DENSITY OF O (cm^{-3})
53
01C103-110S

Figure 1.

abundance of 250 cm NTP which can be considered as a rather definite upper limit (Dunham 1952) no evidence could be obtained for the development of an ozone concentration peak at some altitude above the surface of Mars. On the basis of the present work, therefore, it appears that existence of an ozone layer in the atmosphere of Mars can be denied.

REFERENCES

Detwiler, C.R., D.L. Garrett, J.D. Purcell, and R. Tousey, The intensity distribution in the ultraviolet solar spectrum, Ann. de Geophysique, Tome 17, 263, 1961.

Dunham, T., Spectroscopic observations of the planets at Mount Wilson, in The Atmospheres of the Earth and Planets, ed. G.P. Kuiper, University Chicago Press p. 296, 1952.

Gast, P.R., in Handbook of Geophysics, Revised Edition, The MacMillan Co., New York, chapter 16, p. 25, 1961.

Inn, E.C.Y., and Y. Tanaka, Ozone absorption coefficients in the visible and ultraviolet regions, in Ozone Chemistry and Technology, Advances in Chemistry Series 21, American Chemical Society, p. 263, 1959.

Johnson, F.S., The solar constant, J. Meteorol. 11, 431-439, 1954.

Kaplan, L.D., G. Munch, and H. Spinrad, An analysis of the spectrum of Mars, Astrophys. J., 139, 1-15, January 1964.

Kaufman, F., Reactions of oxygen atoms, in Progress in Reaction Kinetics, ed. G. Porter, Pergamon Press, New York 1961.

Marmo, F.F., and P. Warneck, Photochemical processes in the atmosphere of Mars, in Final Report on Laboratory and Theoretical Studies in the Vacuum Ultraviolet for the Investigation of Planetary Atmospheres, Contract NASw-124, Technical Report No. 61-20-N. Geophysics Corporation of America, Bedford, Mass., 1961.

REFERENCES (Cont'd.)

Paetzold, H.K., On the problems of martian ozonosphere, Mémoirs de la Société Royale des Sciences de Liège, Tome VII, pp. 452-459, 1963.

Schilling, G.F., Limiting model atmospheres of Mars, Report R-402-JPL, The Rand Corporation, Santa Monica, Cal., 1962.

Shimizu, M., Vertical distribution of neutral gases on Mars, Report Ionosphere Space Res. Japan, Vol. XVI, 425 (1963).

Watanabe, K., M. Zelikoff, and E.C.Y. Inn, Absorption coefficients of several atmospheric gases, AFCRL Technical Report No. 53-23, Geophysical Research Paper No. 21, Geophysics Research Directorate Cambridge, Mass., 1953.